2012

Characterization and rejection of noise from in-cylinder pressure traces in a diesel engine

Koustav Dey
University of Windsor

CHARACTERIZATION AND REJECTION OF NOISE FROM IN-CYLINDER PRESSURE TRACES IN A DIESEL ENGINE

by

Koustav Dey

A Thesis
Submitted to the Faculty of Graduate Studies
through the Department of Electrical and Computer Engineering
in Partial Fulfillment of the Requirements for
the Degree of Masters of Applied Science at the
University of Windsor

Windsor, Ontario, Canada
2012

CHARACTERIZATION AND REJECTION OF NOISE FROM
IN-CYLINDER
PRESSURE TRACES IN A DIESEL ENGINE

by

Koustav Dey

APPROVED BY:

_____

Dr. Behnam Shahrrava
Department of Electrical and Computer Engineering

_____

Dr. Ming Zheng
Department of Mechanical, Automotive and Materials Engineering

_____

Dr. Xiang Chen
Department of Electrical and Computer Engineering

_____

Dr. Faouzi Ghrib
Department of Civil and Environmental Engineering

_____

Dr. Robert Muscedere, Chair of Defense
Department of Electrical and Computer Engineering

16th May, 2012

AUTHOR'S DECLARATION OF ORIGINALITY

I hereby certify that I am the sole author of this thesis and that no part of this thesis has been published or submitted for publication.

I certify that, to the best of my knowledge, my thesis does not infringe upon anyone's copyright nor violate any proprietary rights and that any ideas, techniques, quotations, or any other material from the work of other people included in my thesis, published or otherwise, are fully acknowledged in accordance with the standard referencing practices. Furthermore, to the extent that I have included copyrighted material that surpasses the bounds of fair dealing within the meaning of the Canada Copyright Act, I certify that I have obtained a written permission from the copyright owner(s) to include such material(s) in my thesis and have included copies of such copyright clearances to my appendix.

I declare that this is a true copy of my thesis, including any final revisions, as approved by my thesis committee and the Graduate Studies office, and that this thesis has not been submitted for a higher degree to any other University or Institution.

ABSTRACT

Diesel engine in-cylinder pressure analysis is important for engine research and diagnosis. It has been a subject of interest right from the inception of internal combustion engines. Engine cylinder pressure measurements provide insight into the combustion process and the accuracy of these measurements governs the quality of analyses of different combustion modes of the engine. Since the in-cylinder pressure increases abruptly after the start of combustion, non-flush mounting of the pressure transducer creates standing/resonant waves in the access passage which severely affect the recorded pressure fidelity by introducing undesired noise. The challenge is to get rid of these pressure pulsations and characterize the unaccounted noise which can lead to erroneous determination of different combustion parameters and characteristics.

This work focuses on online filtering of the noisy pressure data so as to obviate the need of any post-processing for combustion and noise analysis. An online filtering algorithm is defined which is a combination of a five-point moving average filter and a forward and reverse Butterworth digital filter. The filter is tested for its robustness over different engine operating conditions such as engine load, speed, boost etc. The cut-off frequency of the filter is determined on a cycle-by-cycle basis using an algorithm based on the power spectral density of the pressure signal. The noise component is segregated from the pressure trace by means of pressure decomposition technique and the peak noise power is attributed to the access passage resonance frequency. Further development of this approach can be used to achieve optimal combustion control by means of the development of optimal injection strategies in order to fulfill emission reduction and performance requirements in Diesel engines.

DEDICATION

This thesis work is dedicated to my beloved parents. Without their unconditional support all throughout my research endeavor, it would have been impossible to complete this work with success.

ACKNOWLEDGEMENTS

I hereby extend my deepest gratitude and acknowledgement to everyone who helped me complete my Master's thesis successfully. I would specially thank my supervisors Dr. B. Shahrrava and Dr. M. Zheng, without whose guidance and support this thesis would have not been a success. I would also like to thank my thesis committee members Dr. X. Chen and Dr. F. Ghrib whose suggestions were effective in making my research more fruitful. I hereby thank all the team members of Clean Diesel Engine Laboratory for their continuous support during my research work.

Koustav Dey
Windsor, Ontario, Canada
May 2012

TABLE OF CONTENTS

LIST OF FIGURES

LIST OF TABLES

NOMENCLATURE

CA	Crank Angle
CA50	Crank Angle of 50% heat released
CO_2	Carbon dioxide
EOC	End of Combustion
EVO	Exhaust Valve Opening
FFT	Fast Fourier Transform
FIR	Finite Impulse Response
H_2O	Water
HCCI	Homogeneous Charge Compression Ignition
HRR	Heat Release Rate
IIR	Infinite Impulse Response
IMEP	Indicated Mean Effective Pressure
IVC	Inlet Valve Closure
LTC	Low Temperature Combustion
N_2	Nitrogen
NI	National Instruments
O_2	Oxygen
PSD	Power Spectral Density
RPM	Revolutions per minute

R_m	Universal Molar Gas Constant
SAES	Synthetic Atmospheric Diesel Engine Simulation
SOC	Start of Combustion

1. INTRODUCTION

1.1. Motivation

Diesel engine in-cylinder pressure analysis is important for engine research and diagnosis. Among its many applications, combustion and noise analysis based on the first law of thermodynamics is the most important. A noisy cylinder pressure data can obscure the heat release rate calculation, a parameter that is derived from the acquired cylinder pressure. Heat release analysis of a combustion trace can be used to (a) validate mathematical models for engine simulation, (b) develop new combustion systems (c) analyze alternative fuel burning and (d) study new fuel injection strategies. In order to explore these areas with high fidelity, reliability of the heat release rate and hence accuracy of the cylinder pressure trace is highly desirable. The challenge here is to eliminate the pressure pulsations and characterize the unaccounted noise on a cycle-by-cycle basis. Many studies show that pollutant emission reduction can be achieved by means of an optimal combustion control strategy.

1.2. Objective and approach

The principal objective of this work is to eliminate the unaccounted noise from the in-cylinder pressure trace and characterize the noise signal. Although there are multiple sources of noise which can interfere with the cylinder pressure trace, the principal sources of noise are identified as part of this work and the power spectral density of the noise curve is plotted. In addition to this, the filtering algorithm has to be stressed upon because the noisy pressure data cannot be reconstructed by using a simple filter.

One approach to reject the unaccounted noise from in-cylinder pressure trace could be to design a suitable filter. The filter parameters have to be determined keeping in mind that the filter has to work online i.e. on a cycle by cycle basis and has to be tested over all engine operating conditions to prove its robustness. The in-cylinder pressure trace is decomposed into the motoring, combustion-only and noise signal components. Spectral analysis of the pressure trace is carried out by using Fast Fourier Transform (FFT) to obtain the frequency components

of the signal. It is shown that, under certain conditions, resonance phenomenon inside the cylinder chamber can be an important aspect in combustion noise analysis [11]. The acquired cylinder pressure data is simulated by using SAES [20] to determine the acoustic wave speed inside the cylinder chamber and the concentration of the gaseous mixture. These parameters are used to validate the peak noise frequency with the access passage resonance frequency.

1.3. Thesis organization

This thesis work is divided into six chapters.

Chapter 1: This chapter covers the motivation, objective and approach and the thesis organization.

Chapter 2: Background study and Literature Review: This chapter provides basic ideas about the different components and terms necessary and associated with this research work such as pressure transducer system, adapter, filter types and parameters, sources of noise associated with diesel engine etc. This part also shows a comparative study of the filters used so far in the literature and their drawbacks are pointed out. The challenges are identified and the most suitable approach is defined.

Chapter 3: Study of important parameters and filters: This chapter briefly familiarizes with important engine related parameters such as heat release rate (HRR) and indicated mean effective pressure (IMEP). This chapter also includes a discussion on the general characteristics and types of filters. A brief discussion is done on IIR and FIR filters and the choice of Butterworth filter for this work is justified.

Chapter 4: Empirical set up: In this chapter, the experimental set up is shown. This chapter includes a brief discussion about the two research engines in the laboratory that are used for this research work. It also includes a brief discussion on pressure transducer system and charge amplifier used in the laboratory. A complete block diagram for the cylinder pressure acquisition and display system is included in this chapter as well.

Chapter 5: Design of filter: Results and Discussion: This chapter shows the results of the filtering algorithm on the raw unfiltered pressure data on a cycle-by-cycle basis. The simulation of the cylinder pressure diagram is used to validate the peak noise frequency for the single cylinder engine (since the access passage length is known) with the access passage frequency. A pressure decomposition technique is introduced which helps in the characterization of the resonance noise and combustion noise analysis.

Chapter 6: Conclusion and future work: In this chapter, the concluding remarks on the noise attenuation and filter design are expressed. The pros and cons of the filtering algorithm used in this thesis work are discussed in brief. Future work in terms of the development of optimal fuel injection strategies in order to meet the sound quality requirements in diesel engines is proposed.

2. BACKGROUND STUDY AND LITERATURE REVIEW

This chapter will review the previous work, different methodologies used for the application of signal processing on in-cylinder pressure trace of diesel engines and the improvements achieved eventually in terms of noise rejection. The first part of the review identifies the key areas of combustion and noise analysis and the possible factors behind the problem. Non-flush mounting of the pressure transducer is a significant contributor of noise in the in-cylinder pressure trace. Due to an abrupt increase in cylinder pressure after the start of combustion, non-flush mounting of the pressure transducer creates standing/resonant waves in the access passage which severely affect the recorded pressure fidelity by introducing unwanted noise. Fig 2.1 shows a cycle of unfiltered cylinder pressure trace measured from a non-flush mounted pressure transducer. High frequency oscillations obscure the cylinder pressure trace.

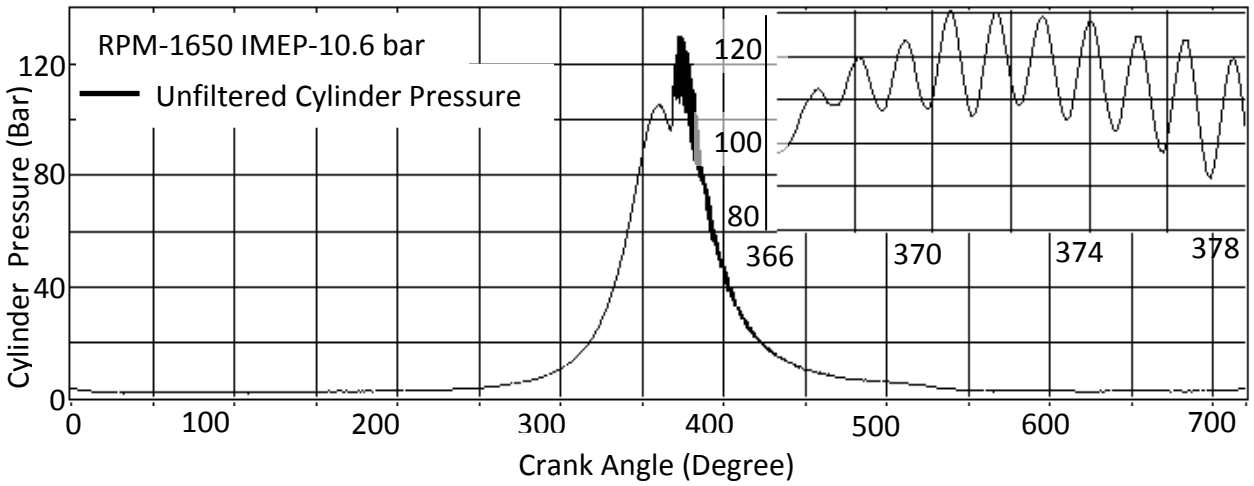

Fig 2.1: Unfiltered Cylinder Pressure trace (one cycle)

This review stresses upon the research done so far in order to find the best possible position of transducer installation and also determination of the most suitable type of transducer for a noise free pressure recording. An approach of modification of the access passage by designing a transducer adapter system [3] has been used in the literature to nullify the effect of the resonance passage. An alternative option is to use an appropriate filter to reject the noise from in-cylinder pressure trace. Therefore, a review of the different types of filters used in the

literature is included in this section and a comparison is made between the results obtained highlighting the limitations and scope of improvement.

2.1. Position and type of the pressure transducer

The frequency response of a pressure transducer is an important factor towards the choice of transducer. The highest frequency up to which the transducer transmits information without any significant modification is usually a fraction of the first natural frequency of the device [4]. Non-flush mounting of the transducer leads to further reduction of the frequency response. If the cylinder chamber and the transducer diaphragm are coupled through a passage, the natural frequency of the passage should be higher than the minimum desired frequency of interest of the transducer. The combined frequency response of the pressure transducer and the recording system should be flat up to 10 kHz and should not fall steeply at higher frequencies [1]. Strain gauge, capacitance and piezo-electric transducers have frequency responses in this order. However, electromagnetic transducers are not suitable for this purpose as most of the high frequency components are lost in the process of obtaining a pressure-time display [1]. Lyn et al [1] investigated the responses of all three types of transducers to a pressure step input signal in shock tube. It was observed that capacitance and strain gauge transducer responses include some low frequency oscillations whereas piezo-electric transducer response was almost flat in the range of interest. These transducers have the most desirable technical specifications regarding bandwidth, thermal characteristics, robustness, accuracy, durability and size [15]. Moreover, these transducers have a temperature range of up to 620 K, much higher compared to 423 K of piezo-resistive sensors [16]. Therefore, piezo-electric transducers are mostly used for recording in-cylinder pressure.

A non-flush mounted pressure transducer may induce a substantial error in the absolute pressure value and also a phase difference as a result of the time required by the pressure wave to travel the distance from the combustion chamber through the duct to the transducer position [2]. Hountalas et al. [2] observed that duct geometry and engine speed affect the cylinder pressure diagram error significantly whereas the pressure diagram remains

undisturbed by the changes in engine load. Hountalas et al. [2] showed that the peak pressure error increases with an increasing duct length, decreasing duct diameter and an increasing engine speed. Access passage diameter equal to that of the sensor helps to eliminate Helmholtz resonance [16]. A transducer adapter system with a natural frequency higher than the maximum frequency content of the pressure signal can eliminate noise interferences [3]. An alternative way to attenuate the noise interferences is to use an adaptive digital filter to filter the noisy cylinder pressure trace.

The mechanical vibration noise is attenuated by means of acceleration compensated sensors and bulk of the electrical noise can be reduced by proper insulation of the system transducer-cable-charge amplifier. But, the significance of the errors discussed here depends on the kind of analysis. Indicated mean effective pressure (IMEP) is very sensitive to crank-angle phasing error and thermal shock but rather insensitive to absolute pressure referencing and random noise whereas heat release analysis is sensitive to all the errors discussed thus far. The recorded pressure trace has to be processed to extract reliable information. Therefore, a more reliable approach would be to use a filter with suitable specifications to reject the unwanted frequency components and allow the information signal components to pass through.

2.2. Type of filters used and their characteristic parameters

In-cylinder pressure analysis is usually a four-step process consisting of level correction, angle-referencing, cycle-averaging and filtering. This study stresses upon the last two steps. F.Payri et al. [5] used an adaptive low-pass finite impulse response (FIR) filter for online analysis of the pressure signal, cut-off frequency being determined by taking into account the signal-to-noise ratio of the signal (based on a cut-off harmonic map). The authors determined the cut-off harmonic as the point where the average cycle harmonics converges with the non-cyclic harmonics, attributable to signal noise and cycle-to-cycle variations. They used Remez algorithm [17] for obtaining the filter order and the coefficients. It was observed that the filter order increases with increasing load and speed.

R.Douglas et al. [6] used simple hardware electrical low-pass filter to attenuate the noise components from the pressure trace and applied timing correction to account for any group delay caused by the online filtering. A center-weighted moving average filter was also proposed for the post-processing of the recorded pressure although Shi et al. [7] observed that a moving average filter might not eliminate duct resonances properly whereas sharp pressure fluctuations owing to premixed combustion can be also distorted. Moreover, the smoothing capability of the moving average filter depends on the sampling interval. F.Payri et al. [9] chose cut-off frequency of the filter such that there is no statistical difference between the signal and noise at that point.

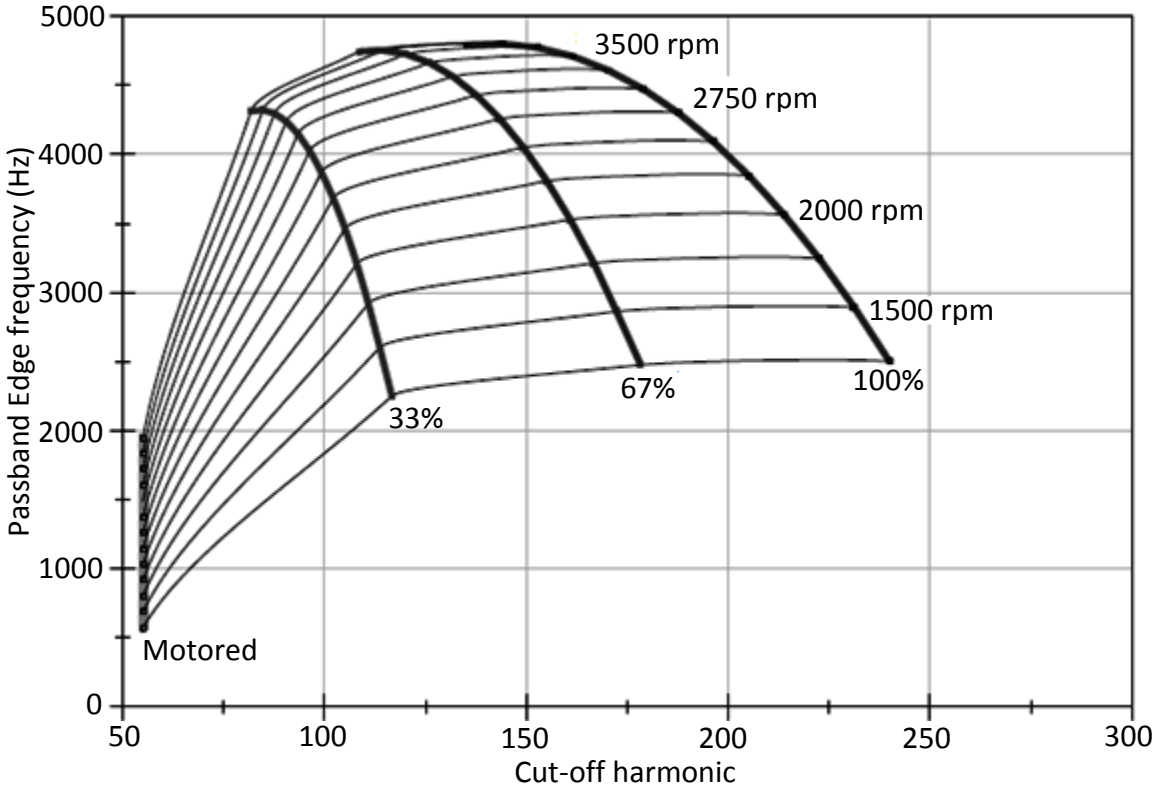

Fig 2.2: Map for Cut-off frequency (Adapted from [5])

The challenge is to determine the pass-band edge (corner) frequency adaptively so as to segregate the noise and the information frequency components. Different methods have been studied and employed in the literature in order to determine an appropriate cut-off frequency of the filter. Direct elimination of high frequency band can create overshoots in the pressure signal (Gibbs effect) [5] which results in non-negligible errors in heat release calculation. Shi et

al. [7] suggested the use of Hanning window (window-sync filter), defined between two cut-off frequencies viz. stop-band initial frequency and stop-band final frequency, to mitigate the Gibbs effect by smoothing the transition (increasing the roll-off). Savitzky et al. [8] proposed a slightly more complicated but accurate filtering procedure based on least squares fit, also known as Savitzky-Golay filter.

Table 2.1: Comparative analysis of the filters used for noise attenuation

Proposed Online Filters	Comments
A variable-order low-pass FIR filter by F.Payri et al. [5]	The cut-off is determined based on a preset frequency cut-off map and therefore is non-adaptive. Number of samples (1440) per cycle is too low. The operating range of the engine was 1000-3000 rpm at all loads.
A low-pass hardware filter with corner frequency equal to half of sampling frequency by Douglas et al. [6]	This choice of cut-off frequency is not accurate as noise components might be present below the cut-off range determined used this procedure.
A mapped cut-off frequency filter by Martin et al. [9]	The stop-band initial frequency varies linearly only with engine speed from 1250 rpm to 4000 rpm. However, this does not take into consideration the variation of the frequency components with engine load.
Ithaco electronic order 8 Bessel filters by J.A.Eng. [14]	The cut-off frequency was chosen to be equal to the first circumferential mode frequency. This is more useful for offline analysis rather than online pressure analysis.

F.Payri et al. [9] found that sharp heat release peaks caused by premixed combustions were smoothed and therefore suggested that smoothing methods are not frequency sensitive and hence not recommended. Kosarev et al. [10] proposed an optimal Weiner filter with an assumption that 90% of the Fourier spectrum constitutes of noise with constant intensity; the cut-off frequency being the point where the ratio between the harmonic level and the standard deviation of the noise is unity.

To summarize, a wide variety of filtering options have been used so far in order to eliminate the high frequency noise from the in-cylinder pressure trace. The general idea is smoothing is not a

feasible filtering option because of its poor performance in the frequency domain. Therefore, a filter with desirable properties in the time domain as well as in the frequency domain is of prime importance. Table 2.2 illustrates a comparative study of the filters used in the previous works.

2.3. Identification of different sources of noise from the in-cylinder pressure trace

F.Payri et al. [11] presented the concept of pressure signal decomposition in order to perform an improved combustion noise analysis. F.Payri et al. [11] noted that with the increase in engine speed, there is an energy level increase in the low, medium as well as high frequency components of the cylinder pressure signal. The authors concluded that sound quality of combustion noise is highly correlated with the combustion chamber resonance signal energy content relative to that in the pseudo-motored signal.

Asad et al. [12] stated that the quality of the pressure data from a non-flush mounted transducer can be improved by accounting for the access passage resonance frequency given by $f_n=c/4L$ where 'f_n' is the passage resonance frequency in Hz, 'c' is the speed of sound in m/s and 'L' is the length of the access passage in meters. While analyzing the pressure data in the frequency domain, the transient angular-speed variation has to be accounted for so as to convert the data from the 'crank angle domain' to the 'time domain' which can add significantly to the computational overhead. Due to the variation of the pressure frequency spectrum with change in engine speed, the usual practice in the industry is to set the minimum filter cut-off frequency to at least 100 times the cylinder firing frequency [12]. Hirose [13] stated that the pressure oscillations can be considered acoustic in nature since the amplitude of the fluctuations are small relative to mean cylinder pressure.

2.4. Challenges in filter design

There are various challenges in the process of designing a filter to suit the requirements of the diesel engine in terms of preserving vital information in the cylinder pressure trace. Usually, all electrical filters induce a certain amount of phase shift in the filtered output. A simple phase-

less/zero-phase filter is not an optimum solution to this problem. The reason behind this is an abrupt increase in the pressure trace after the start of combustion. However, even a zero-phase digital filter fails to track this abrupt increase in the cylinder pressure and the consequent shift with respect to the original trace is non-negligible. The designed filter has to be smart enough to make an approximation of the start of combustion and modify the filtered output accordingly so as to eliminate this apparent shift.

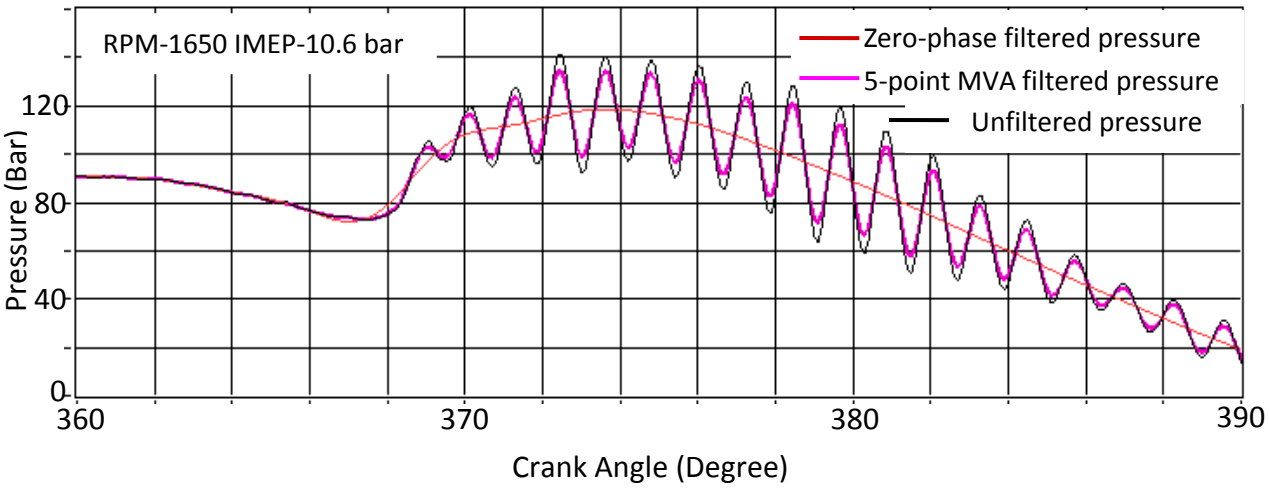

Fig 2.3: Shift in the filtered pressure due to abrupt increase in pressure due to combustion

Fig 2.3 shows the output of a five-point moving average filter and a zero-phase Butterworth filter to a noisy pressure trace. Determination of essential filter parameters such as cut-off/corner frequency, order of the filter, pass-band characteristics etc. is also a point of concern especially when the filter is operating online. Since the frequency spectrum of the pressure trace changes with the variation of engine speed and load, having a preset/pre-determined cut-off frequency for all modes of operation is not the proper approach. Therefore, a more appropriate approach is to adopt an adaptive mechanism for selecting the cut-off frequency for the filter on an online basis. The type and bandwidth (pass-band and transition band) of thex filter has to be determined based on frequency response of the cylinder pressure trace. Since most of the noise and resonant frequency components are predominantly in the high frequency zone, a low-pass filter can attenuate the noise components. Filter type is also important because different filters have different roll-off factors and pass-band ripples. Impulse response of the filters can also be a determining factor in the choice of filter.

3. STUDY OF IMPORTANT PARAMETERS AND FILTERS

The cylinder pressure trace is an important source of information in order to carry out noise and thermodynamic analysis (usually combustion analysis). It provides a variety of information e.g. heat release rate (HRR), start of combustion (SOC), IMEP (Indicated Mean Effective Pressure), maximum rate of pressure rise, peak cylinder pressure and crank angle corresponding to peak cylinder pressure, end of combustion (EOC) etc. Since many of these parameters are derived from the in-cylinder pressure trace and heat release rate, a high fidelity pressure recording is essential for correct analysis of cylinder pressure in diesel engines. Use of an electrical filter to attenuate the cylinder pressure noise results in a phase shift that can affect thermodynamic analysis e.g. one degree CA shift in a single pressure cycle can cause an error up to 5% in the IMEP [12]. Errors in IMEP are primarily caused by thermal shock, crank angle phasing errors and transducer sensitivity [18]. Therefore, even before filtering of the pressure data, care has to be taken to acquire pressure data with high fidelity so as to nullify the effect of thermal shock and CA phase errors.

3.1. Heat Release Rate

Heat Release Rate (HRR) analysis is used in diesel engines to obtain vital information regarding the performance and emission characteristics of the engines. Heat Release formula can be derived from the first law of thermodynamics for an open system taking into consideration the effects of heat transfer, crevices, blow-by and fuel injection effects [12,19]. The gross heat release rate (measured from IVC to EVO) is given by

$$dQ_{gr} = dU + \delta W + \sum_i h_i dm_i + \delta Q_{ht} \tag{3.1}$$

where, dQ_{gr} is the fuel chemical energy released due to combustion, dU is the change in sensible energy, δW is the piston work done, dQ_{ht} is the heat transferred to the chamber walls, the mass flux term $\sum_i h_i dm_i$ is the flow across the system boundary. However, assuming the cylinder chamber contents as single zone, neglecting the heat transfer to the chamber wall,

crevice volume and effects of fuel injection [12], the apparent or net heat release [19] during combustion can be given by

$$dQ_{app/net} = dQ_{gr} - dQ_{ht} = \frac{1}{\gamma - 1}\left[\ \gamma\ pdV + Vdp\ \right] \tag{3.2}$$

where, p is the in-cylinder pressure, V is the instantaneous cylinder volume and γ is the adiabatic coefficient. This formula was used to calculate the value of the apparent heat release from the pressure data. It can be clearly seen that the heat release rate term has a derivative of the pressure term and therefore any error or high frequency noise in the measured cylinder pressure will appear with increased distortion in the apparent heat release term. The calculation was done on a crank angle basis and the value of the adiabatic coefficient was assumed to be constant over the cycle. Fig 3.1 shows the effect of cylinder pressure noise on Heat Release Rate. Attenuation of high frequency noise from the heat release curve allows the determination of different thermodynamic parameters with greater fidelity.

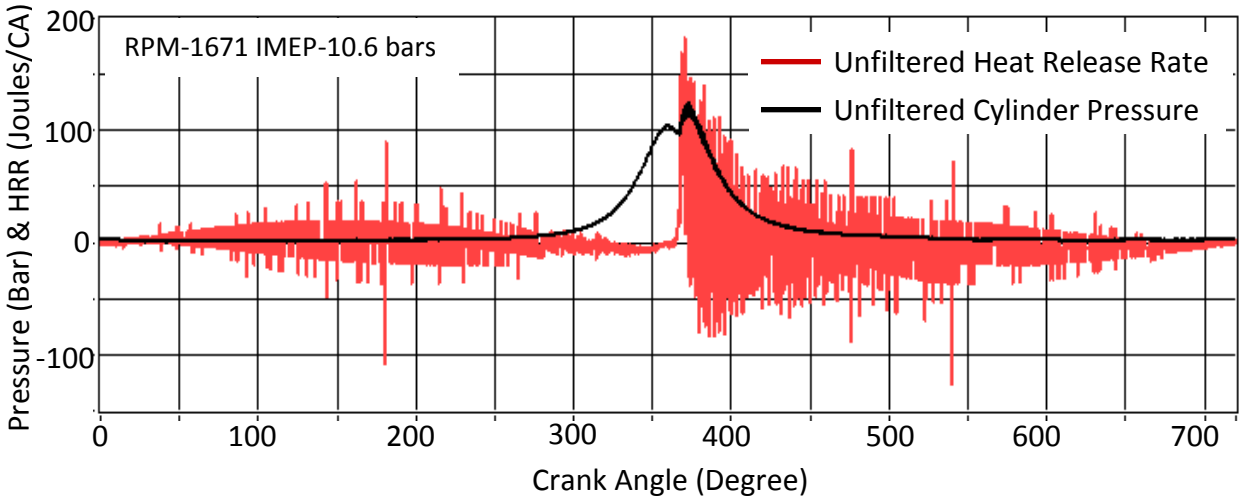

Fig 3.1: Unfiltered pressure and heat release curves

3.2. Indicated Mean Effective Pressure (IMEP)

Indicated Mean Effective Pressure (IMEP) is defined as the measure of the indicated work or the power output per cycle i.e. the sum total of the compression stroke work and the expansion stroke work. It is given by

$$imep = \frac{W_{c,i}}{V_d} \tag{3.3}$$

where, $W_{c,i}$ is the sum of the compression stroke work and the expansion stroke work and V_d is the displacement volume of the cylinder. However, this corresponds to gross IMEP measurement whereas if work done in all the four strokes of the engine is taken into consideration, the measured IMEP is called net IMEP. The formula for the measurement of IMEP [19] is given by

$$imep = \frac{\int p_{avg} dV}{V_d} \tag{3.4}$$

where, p_{avg} is the average pressure over crank angle interval (if measurement is done in crank angle domain), V_d is the displacement volume of the cylinder and dV represents the change in the cylinder volume over the crank angle interval. It is evident from Eq. 3.4 that noisy pressure data can obscure the IMEP calculation and thereby hamper the cylinder pressure analysis.

3.3. Study of filters suitable for cylinder pressure signal processing

3.3.1. Filters

Filtering is a class of signal processing, the defining feature of filters being the complete or partial suppression of some aspect of the signal. Most often, this means removing of some frequencies and not others in order to suppress interfering signals and reduce background noise. Filters are characterized by the following important parameters.

Cut-Off Frequency (fc): Also referred to as the corner frequency, this is the frequency or frequencies that define(s) the limits of the filter range(s). It is the desirable cut-off point for the filter.

Stop Band: The range of frequencies that is filtered out.

Pass Band: The range of frequencies which is let through and recorded.

Transition Band: The range of frequencies between the pass-band and the stop-band where the gain of the filter varies with frequency.

Digital filters are preferred in this case as they directly implement the mathematical algorithm on the sampled or digitized signal. Primarily, digital filters can be broadly classified into two categories namely Infinite Impulse Response (IIR) filter and Finite Impulse Response (FIR) filter.

3.3.1.1. IIR (Infinite Impulse Response) Filter

IIR filter has an impulse response function that is non-zero over an infinite length of time. It uses feedback and therefore the phase shift is a non-linear function of frequency. IIR filter is derived from analog filters and make poly-phase implementation possible. Another salient feature of IIR filters is that they have sharper roll-off compared to FIR filters of the same order. IIR filters require less computational memory compared to FIR filters. High computational efficiency and short delays make IIR filters an attractive alternative. IIR filters can be set up as online calculation channels for real-time digital filtering.

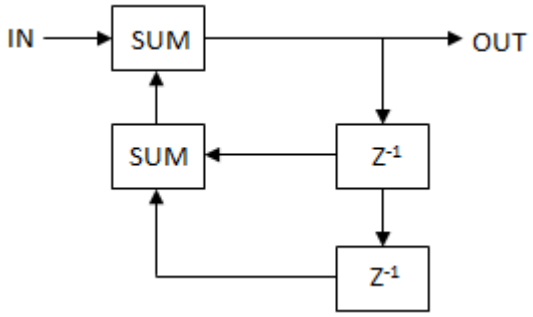

Fig 3.2: Sample IIR filter block diagram

3.3.1.2. FIR (Finite Impulse Response) Filter

An FIR filter has an impulse response of finite duration i.e. it settles to zero in finite time. Since, the filter does not use feedback, the phase shift is linear but it requires more computing power than an IIR filter. The most significant advantage of FIR filters is their linear phase characteristics. FIR filters have better delay characteristics compared to their IIR counterparts but they require more memory. FIR filters do not rely on feedback i.e. they are dependent only on the inputs. FIR filters are stable compared to IIR filters when subject to distortion

adjustments. They are non-recursive and are not suitable for simulating analog filter responses. FIR filters are available only in software; they cannot be set up as calculation channels and must be applied as transformations once the acquisition is done. An FIR filter requires a very high number of coefficients which should be greater than or equal to at least four times the sampling frequency divided by the lowest cut-off frequency specified.

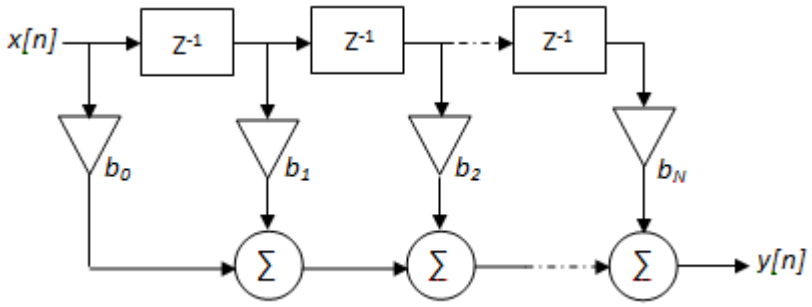

Fig 3.3: A discrete-time FIR filter of order N and containing N+1 taps

In spite of non-linearity of phase, IIR filter is more suitable for this work as compared to FIR filter, because of its low memory requirement and sharper roll-off factor compared to FIR filter of the same order. In addition to that, IIR filters are more suitable for real-time digital filtering. The non-linearity in phase was handled in this work by means of a forward and reverse digital filter which will be discussed in detail in later chapters.

3.3.2. Butterworth filter: Characteristics of IIR Filters

There is a wide variety of IIR filters available such as Butterworth filter, Elliptic (Cauer) filter, Bessel filter, Chebyshev filter etc. Among all these filters, Butterworth has the flattest pass-band response and poor roll-off rate. Chebyshev filter has a steeper roll-off and more pass-band ripple (Type I) or stop-band ripple (Type 2) than a Butterworth filter. Chebyshev filters minimize the error between the idealized and the actual filter characteristics over the range of the filter, but with inherent pass-band ripples. An elliptic filter (also known as Cauer filter) is characterized by an equiripple (equalized ripple) in both pass-band and stop-band. The amount of ripple in each band is independently adjustable and it has the fastest transition in gain

between the pass-band and stop-band, for given values of the ripple (equalized or non-equalized). Bessel filter has the best phase response and the slowest of all roll-off rates. But, a higher order of Bessel filter is required as compared to a Butterworth filter in order to perform the same level of filtering which adds to the complexity.

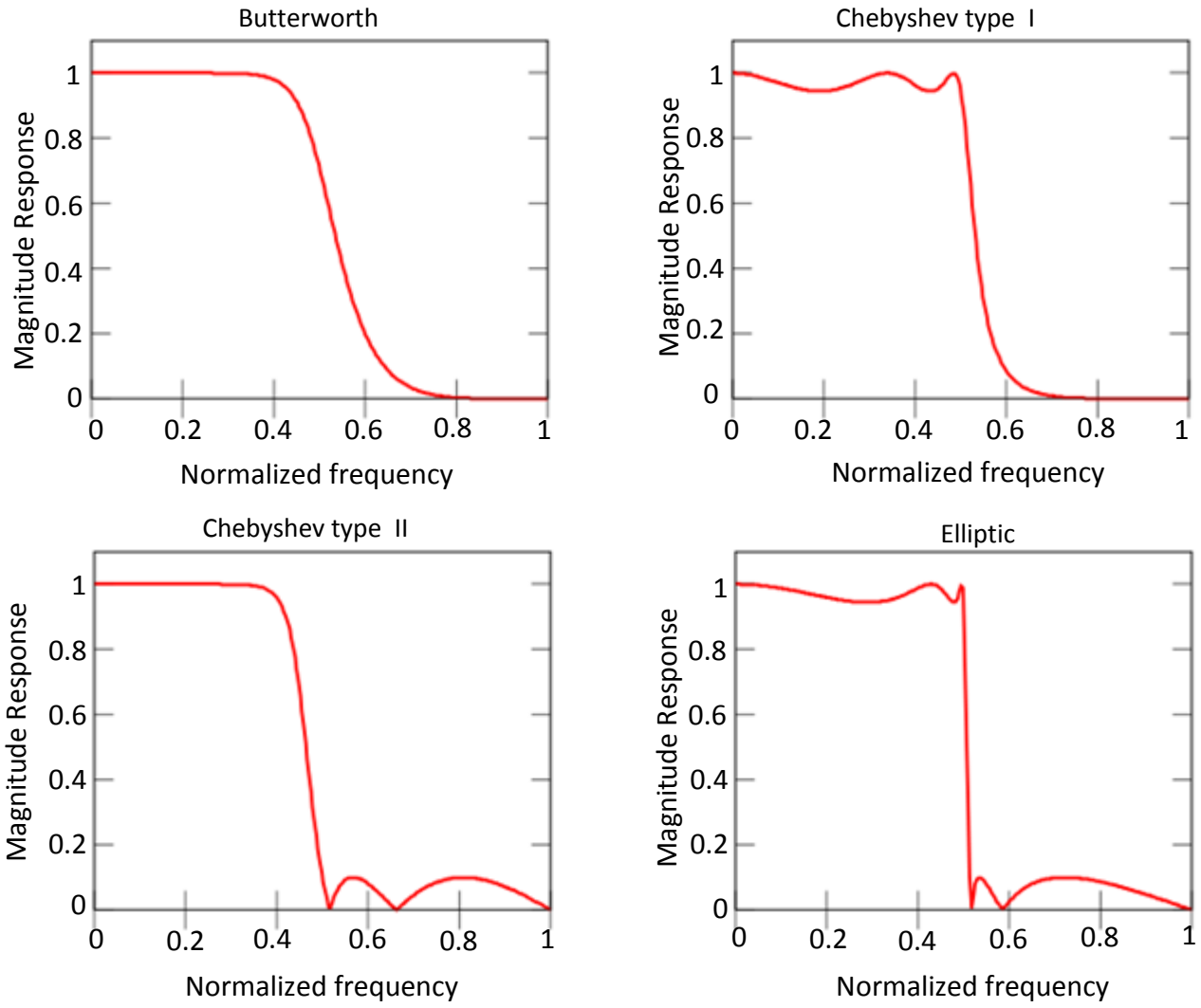

Fig 3.4: Frequency responses of fifth order low-pass IIR filters with cut-off frequency of 0.5 normalized units

As the filter should operate online, the processing time of the filter should be small enough as greater processing time can introduce unnecessary delay in the system. Therefore, the order of the filter has to be chosen in such a way so that the roll-off is not very steep as faster roll-off in frequencies transforms to slower response in the time domain.

4. EMPIRICAL SET-UP

This section explains the layout of the engines used for obtaining empirical results and the mode of connection between the engine chamber and the pressure recording devices and its accessories.

4.1. Single-cylinder Research Engine

The research carried out as part of the thesis work is based on two research engines in the laboratory. One of them is the single-cylinder research engine. One advantage of this engine is that the length of the access passage (glow plug adapter) is known which makes it easier to correlate the peak noise frequency with the access passage frequency. Table 4.1 shows the single-cylinder engine specifications. It is evident that the pressure sensing tip is set back from the chamber surface by 23 mm.

Table 4.1: Single-cylinder research engine specifications

Number of Cylinders	1
Type	4-Stroke
Bore	95 mm
Stroke	105 mm
Connecting rod length	176 mm
Compression ratio	16.2
Duct length	23 mm
Duct diameter	9.6 mm
Injection System	Common Rail

4.2. Ford Puma Research Engine

The Ford Puma engine is a four-cylinder research engine. Majority of the online cylinder pressure analysis work was done on this research engine. This engine is also referred to as the “Box Engine” since both the bore and stroke are equal. Although it has four cylinders, research

is conducted on cylinder number one, which is isolated from the other cylinders. The table below shows the engine specifications.

Table 4.2: Ford Puma research engine specifications

Number of Cylinders	4
Type	4-Stroke
Bore	86 mm
Stroke	86 mm
Connecting rod length	144 mm
Compression ratio	18.2
Injection System	Delphi Common Rail

The major difference between this engine and the single-cylinder engine, given the scope of the project, is that no information is available regarding the mounting scheme of the transducer. Assuming that the analysis done on the single-cylinder engine is valid, the same procedure can be used to back-track an approximate length of the duct (if at all present) through which the transducer is mounted in the Ford engine. This engine has higher compression ratio compared to the single-cylinder engine.

4.3. Pressure Transducer System

The pressure transducers used for pressure acquisition are different for the two engines in the laboratory. The transducer mounted on the single-cylinder engine is Kistler 6052B1 whereas the one mounted on the Ford engine is AVL GU13P. This section explains the working principle and salient features of Kistler 6052B1 and AVL GU13P transducer.

4.3.1. Pressure Transducers

Kistler 6052B1 is a very small pressure sensor with integrated connecting cable. The natural frequency is very high and therefore it is suitable for knock detection. Owing to its high sensitivity, a high precision and good signal-to-noise ratio (SNR) is obtained. It gives a sensitivity

of -20 pC/bar which varies at most by ±0.5% within the temperature range of 200±50 deg C. More specific transducer specifications are shown in the Table 4.3.

Table 4.3: Kistler 6052B1 pressure transducer specifications

Range	Bar	0-250
Sensitivity	pC/bar	20
Natural frequency	kHz	130
Operating temperature range	deg C	-50-400
Overload	Bar	300
Tightening torque	Nm	1.5
Weight, with cable	G	20
Linearity, all ranges at RT	%FSO	≤±0.4
Plug, Ceramic insulator		M4X0.35
Capacitance without cable	pF	5

AVL GU13P is a sensitive piezo-electric pressure transducer that is suitable for combustion analysis of diesel engines via M8 and M10 glow plug bores. It has a high measuring and operating temperature range that is necessary for the cylinder pressure acquisition system. More details of the specifications of the transducer are available in Table 4.4.

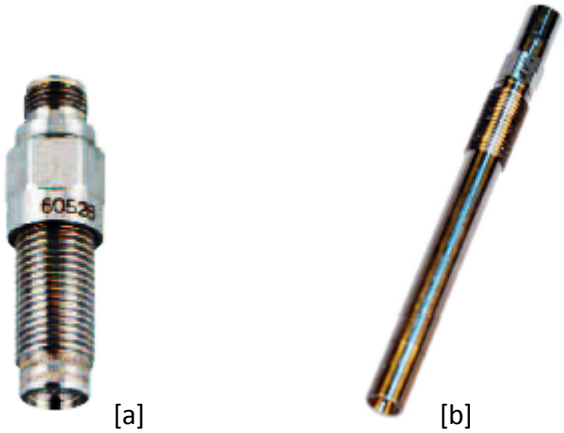

[a] [b]

Fig 4.1: [a] Kistler 6052B1 Pressure Transducer (Adapted from [22]); [b] AVL GU13P Pressure Transducer (Adapted from [23])

Table 4.4: AVL GU13P pressure transducer specifications

Range	Bar	0-200
Sensitivity	pC/bar	15.8
Natural frequency	kHz	130
Operating temperature range	deg C	0-400
Tightening torque	Nm	1.5
Linearity, all ranges at RT	%FSO	≤±0.3

4.3.2. Charge Amplifier

The signal from the pressure transducer is conditioned by a charge amplifier which converts the charge input into an amplified analog voltage output. The charge amplifier used in the laboratory for pressure acquisition in both the engines is Kistler 5010. This charge amplifier has the ability to work reliably with high and low impedance sensors for both dynamic and quasi-static measurements.

Table 4.5: Kistler 5010B0 Dual mode charge amplifier specifications

Measuring Range	Pc	± 10-999000
No. of channels		1
Frequency range	KHz	0-180
Operating temperature range	deg C	0-50
Output signal	V	±10
Voltage	V	89-135
Supply	VAC	115
Mass	Kg	1.27
Connection		BNC neg.
Width	mm	71
Height	mm	184
Depth	mm	129

The time constant of the charge amplifier can be adjusted to either ‘short’ or ‘long’ depending on the type of the test engine. Charge amplifier with short time constant is normally used for pressure acquisition in modern day high speed diesel engines. Usually, piezo-electric principle-based pressure measurement is accompanied by a certain amount of inherent shift in the output signal, which is an undesirable change in the output signal over time. However, the signal drift can be controlled up to a certain limit by operating the charge amplifier in ‘short’ time constant mode or by using a drift compensation circuitry in the charge amplifier [12]. A low-pass filter can also be used within the charge amplifier in order to attenuate undesired high frequency noise accumulated in the cylinder pressure signal. Table 4.5 shows the charge amplifier specifications in detail.

4.4. Pressure acquisition and recording system

In the current experimental set up, the cylinder pressure data is acquired in crank angle domain. Incremental rotary encoders generate a square wave or sinusoidal output signal and enable counters and PLCs to calculate position, speed and distance. There are a few differences between absolute and incremental rotary encoders. Incremental encoders have output signals that repeat over the full range of motion. The position of the incremental encoder is not known just after it is turned on since the output signals are not unique to any singular position. Once an incremental encoder passes an index (either single- or multi-track design), the position information is absolute from that point onwards. However, these encoders are similar in terms of form and issues of count and directional information.

4.4.1. Index-A and Index-Z signals

An optical incremental rotary encoder is installed in the free end of the crankshaft to provide the crank angle data. The encoder shaft is aligned with the crankshaft axis by using a flexible coupling between the encoder shaft and a special mounting fitted into the crank shaft. The importance of the correct alignment of the cylinder pressure data with the corresponding cylinder volume has already been mentioned before. Therefore, in order to achieve this accuracy in terms of alignment, an optical encoder provides the following two outputs:

1. Index ‘A’ signal - It is a TTL signal that corresponds to a fixed angular rotation of the crankshaft. Usually, it is called ‘Index-A’ or clock signal. Optical encoder with an incremental resolution of 0.1 degree CA resolution is used in the current experimental set up. Although the resolution used here is very fine, there remains a scope for the signal to be down-sampled during post- or online processing to obtain data at a coarser resolution (0.5, 0.2 deg CA etc.)
2. Index ‘Z’ signal – It is a TTL signal that is generated once every revolution of the crankshaft and represents a discrete angular position in the engine revolution. This signal is used as the start or event trigger signal in order to start the pressure-data acquisition and is also known as the ‘Index-Z’ signal or simply trigger signal. The start trigger position is usually aligned with either the bottom dead centre (BDC) or the top dead centre (TDC) which eventually makes it obligatory to determine the correct position of TDC and subsequent alignment of the encoder with this position. Several methods have been proposed in the literature regarding the estimation of correct TDC position.

The two index signals generated by the encoder and the amplified signal from the charge amplifier are input to a PC system with a high-speed data acquisition card. The data card installed in the laboratory PC is an M-Series NI-PCI 6229. The data acquisition is externally triggered using the encoder’s Index-Z signal and externally clocked using the encoder’s Index-A signal. The pressure is usually acquired using an analog input channel with a range of 10 V. It can be seen that for a 16-bit ADC resolution, the measurement resolution is 0.61 mV which corresponds to a pressure measurement resolution of 0.012 bar with charge amplifier gain being 1 V=20 bars [12].

4.4.2. Cylinder pressure acquisition system

The tested engine has the piezo-electric pressure transducer non-flush with the cylinder chamber and is fitted into the glow plug adapter on the cylinder head. The output from the pressure transducer is connected to the charge amplifier so as to convert the charge output into amplified analog voltage. Since the signal output from the pressure transducer is of a very

low level, the charge amplifier should be installed as close as possible to the transducer in order to avoid the interference of any external noise including electrical noise. Samples are acquired at 0.1 degree CA resolution (once for every Index-A signal high or tick) and therefore for a 4-stroke engine, 7200 samples are acquired during a single cylinder pressure cycle (one cycle of 4-stroke engine corresponds to two revolutions of the crankshaft i.e. 720 degrees).

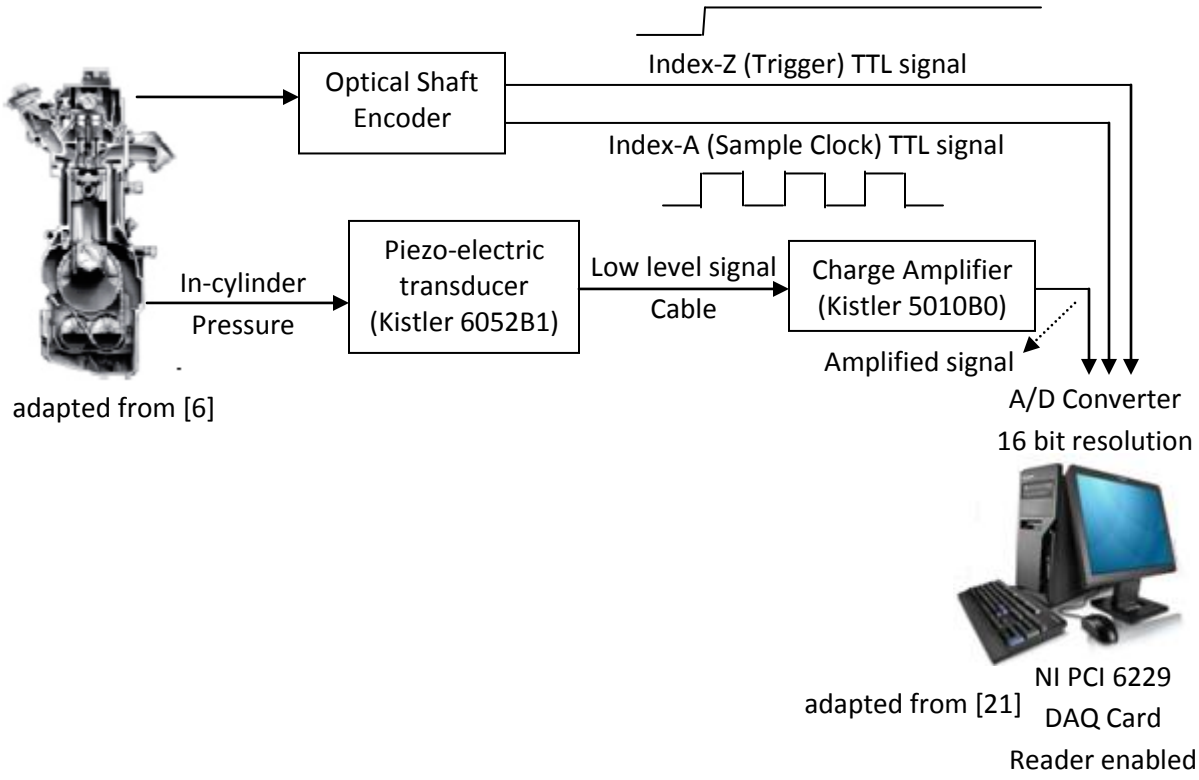

Fig 4.3: Set up for cylinder pressure acquisition

The charge produced by the pressure transducer is amplified to generate an analog voltage signal. Based on the calibration data provided by the manufacturer, the transducer and the charge amplifier have to be matched in order to get accurate measurements. The raw cylinder pressure data along with the corresponding heat release rate (HRR) curve are displayed online by using a NI Labview program.

5. DESIGN OF FILTER: RESULTS AND DISCUSSION

Post-processing of a noisy cylinder pressure data usually involves cycle-averaging followed by the use of a suitable filter with essential parameters so as to remove the unnecessary pressure pulsations from the pressure curve. The design of the filter suitable for this purpose was approached from the point of determination of filter parameters. As mentioned in the previous chapters, cut-off (corner) frequency, type of filter (low-pass or high-pass; IIR or FIR), order etc. are the important filter parameters that have to be determined before designing a filter.

Spectral analysis of a cylinder pressure curve is carried out by using FFT. The cut-off frequency is determined adaptively on an online basis (cycle-by-cycle) as the cylinder pressure signal frequency components change with the change of engine run conditions (e.g. engine speed, engine load, intake pressure or boost etc.). The filter designed here is tested to operate successfully over engine loads (IMEP) in the range of 3 bar to 9 bar and up to an engine speed of 3000 rpm in the laboratory. The filter is able to eliminate noise from the cylinder pressure curve with transient change in the engine speed and load on an online basis.

5.1. Spectral analysis of cylinder pressure: Determination of cut-off frequency

Spectral analysis of the cylinder pressure data is done by first obtaining the autocorrelation function of the cylinder pressure data by means of a Matlab code. In the same code, FFT (Fast Fourier Transform) is used to obtain the power spectral density of the cylinder pressure signal. The number of points (i.e. 16000) used for FFT is chosen to be greater than the number of sample points which is 7200 so that a high frequency resolution is obtained. In this scenario, high frequency resolution leads to a better frequency analysis as it can be confirmed that no frequency peaks are missing. However, as mentioned before, the laboratory is equipped with two diesel engines. Fig 5.1 shows the frequency components of a cylinder pressure cycle in the single-cylinder research engine. The power spectral density (PSD) curve is standardized to the order of 10^7. However, the frequency components observed in this power spectral density diagram are dependent on the engine run conditions such as engine load, speed or boost etc.

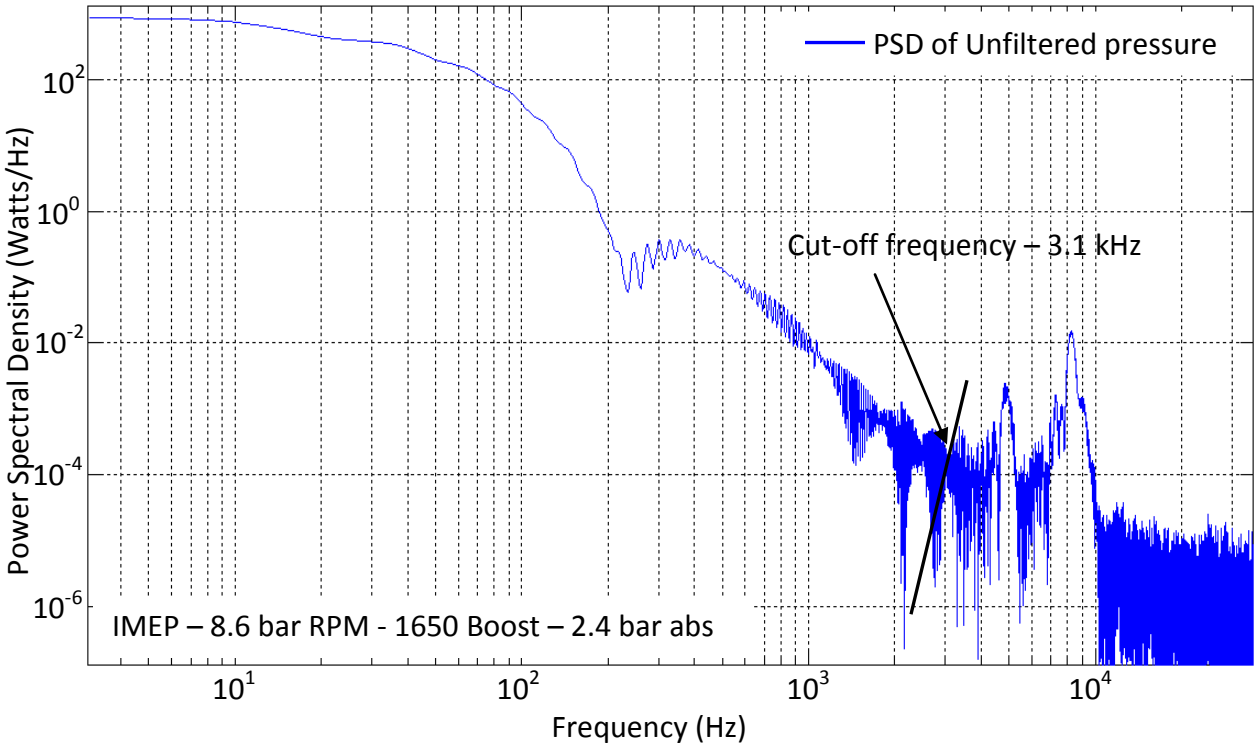

Fig 5.1: Power Spectral Density and cut-off frequency of filter for a cylinder pressure cycle (Single-cylinder engine)

Any variation in these values can lead to changes in the spectral components. This method is used to obtain the power spectral density diagram for all the cylinder pressure traces irrespective of the engine used for the cylinder pressure analysis. Result of similar analysis on the Ford Puma engine cylinder pressure data is shown in Fig 5.2. It can be clearly observed that the peak frequency components in the high frequency zone are different for the two engines.

Since the filter has to operate online, the determination of cut-off frequency has to be done on an adaptive basis. This method of cut-off frequency determination helps in the proper isolation of noise and the information components of the signal. Slope of the power spectral density curve is measured on a point-by-point basis and a ten-point average is calculated in order to have a clear trend of the slope of the curve. Combustion signal spectral components gradually lose power with increasing frequency as shown in Fig 5.1 and 5.2. A sudden increasing trend in the slope on a decreasing PSD curve implies that noise components have started to dominate over the combustion frequency component.

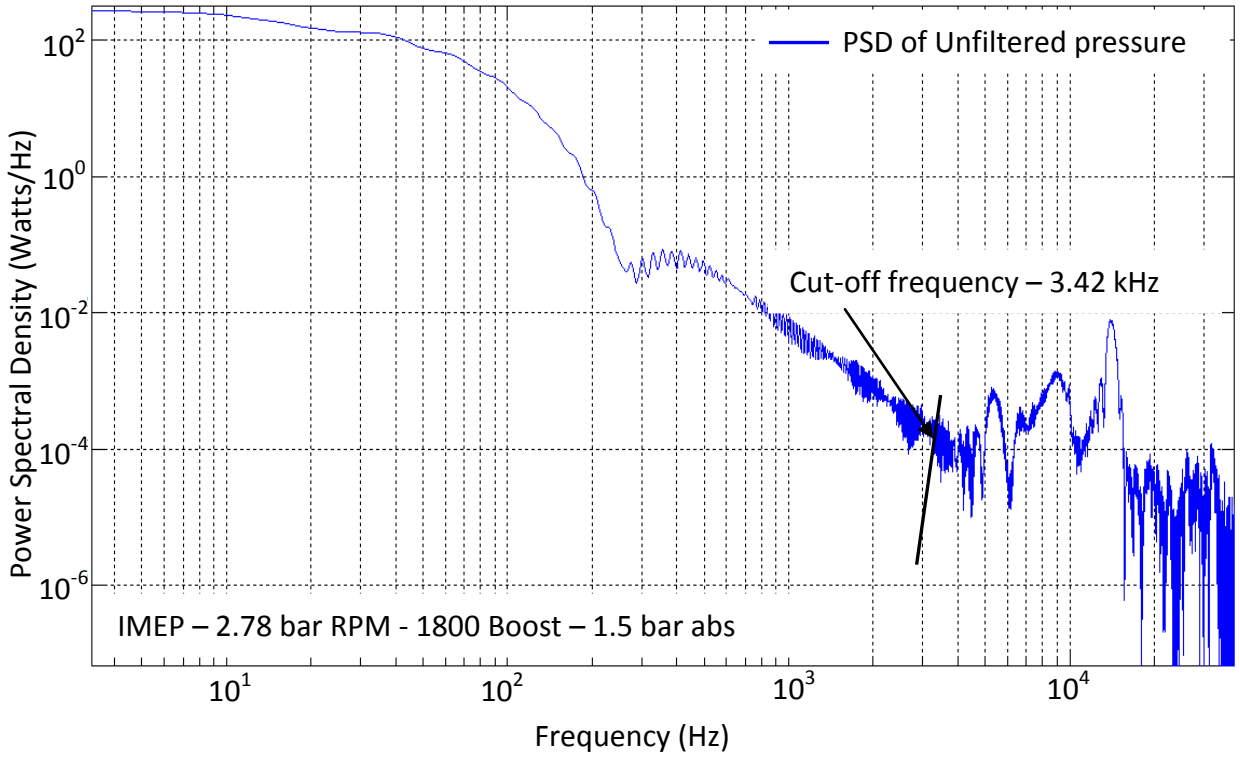

Fig 5.2: Power Spectral Density and filter cut-off frequency for a cylinder pressure cycle (Ford Puma engine)

The determination of the cut-off frequency is done by using the NI Labview code that operates online on a cycle-by-cycle basis. The cut-off frequency of the filter used for the single-cylinder engine pressure cycle as shown in Fig 5.1 is 3.1 kHz and for the Ford engine pressure cycle as shown in Fig 5.2 is 3.42 kHz. These cut-off frequencies correspond to specific engine cylinder pressure cycles and eventually vary from cycle-to-cycle. This provides a better leverage in terms of cycle-by-cycle processing of the engine cylinder data i.e. online analysis when compared to a filter having a preset cut-off frequency. However, the cut-off frequency for the same filter might change drastically with the change in the engine run conditions such as engine speed, load, intake pressure or boost etc.

5.3. Determination of filter type and parameters

It is clearly observed that the spectral components of the cylinder pressure consists of the information components (more clarification is provided in latter sections) in the low and mid frequency zone whereas the high frequency zone is primarily dominated by the unaccounted

noise. Due to an abrupt increase in the cylinder pressure trace when the combustion starts, all digital filters (IIR or FIR) result in an inherent shift at the start of combustion. Therefore, a combination of two filters is used in order to avoid this shift. The filter used in this work for identifying the start of combustion is an IIR filter. The comparative analysis of IIR and FIR filters earlier in Chapter 3 reveals that IIR filter fares better than FIR filters in case of cylinder pressure signal processing. But, one disadvantage of IIR filters as stated before is that they introduce a certain amount of non-linear phase shift in the output signal which is undesirable. Therefore, the filtering algorithm has to remove this non-linearity.

5.3.1. Forward and Reverse Butterworth Filter

A forward and reverse IIR filter is used to filter the raw pressure signal. Among all the IIR filters discussed in Chapter 3, it was evident that Butterworth filter has the best frequency response in terms of roll-off factor and pass-band ripple. Therefore, a forward and reverse Butterworth filter of order 5 (having a moderate roll-off factor) is used for this purpose. Fig 5.3 shows the step response of a 5^{th} order Butterworth filter.

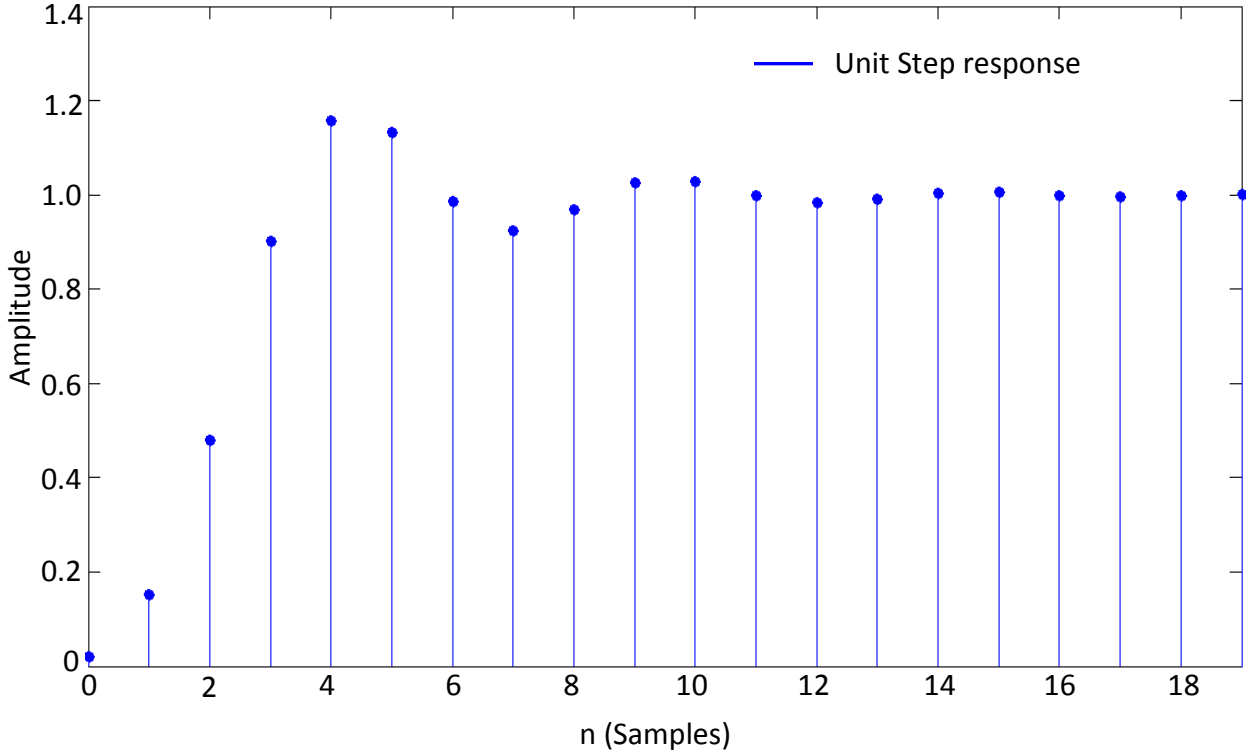

Fig 5.3: Unit Step response of a 5th order Butterworth filter

A lower order filter has less complexity but the transition band is longer which can cause unwanted ripples in the frequency response. A forward and reverse filter is synonymous to a zero-phase filter except that this filter has two separate filtering components. The first component filters the signals samples and then the filtered samples are reversed and fed into the second filter component. The output from the second filtering component is the same as the output from a zero-phase or a phase-less filter. The filtered output is unable to track the raw pressure signal and incurs a certain amount of undesirable shift at the start of combustion. Therefore, use of this filter right from the beginning of the cylinder pressure cycle is not viable. However, the proposed filter switches to the forward and reverse Butterworth filter after the combustion starts. This filter has a variable frequency response as the cut-off frequency is determined on an online basis and thereby varies from cycle to cycle. It is shown later that the proposed filter performs better than a simple zero-phase filter and other filters in tracking the start of combustion from a cylinder pressure curve.

5.3.2. Five-point moving average filter

A weighted five-point moving average filter, a simple low-pass FIR filter, is also used as part of the proposed filter. It is also called Cascaded Integrated-Comb (CIC) filter. Since the high amplitude pressure pulsations are primarily observed after the start of combustion, any random electrical or background system noise appearing in the pressure trace before the start of combustion can be attenuated by a simple moving average filter. An N-point moving average filter generates its output signal *y[n]* by simply taking the arithmetic mean of the input samples *x[n]*. The filtered output *y[n]* is given by

$$y[n] = \frac{1}{N}\sum_{i=0}^{N-1} x[n-i] \tag{5.1}$$

Fig 5.4 and 5.5 show the step response and the frequency response of a five point moving average filter respectively. The frequency response is mathematically described by the Fourier transform of the rectangular pulse and is given by

$$H[f] = \frac{\sin(\pi f N)}{N\sin(\pi f)} \tag{5.2}$$

It is evident from Fig 5.5 that a five point moving average filter is incapable of separating one band of frequencies from another. The moving average filter is an exceptionally good smoothing filter (in the time domain) but an exceptionally bad low-pass filter (in the frequency domain) because of the non-negligible side-lobes in the frequency response.

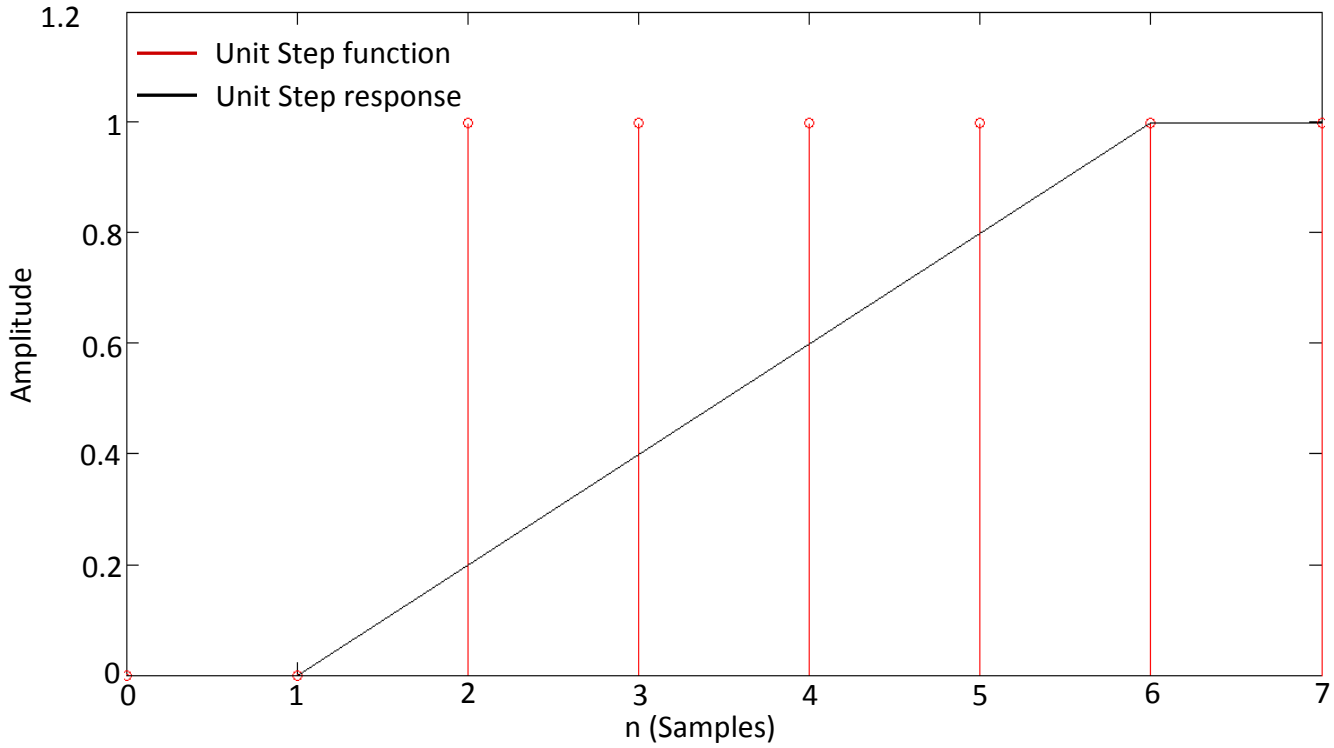

Fig 5.4: Unit Step response of a 5-point moving average filter

This moving average filter has an additional capability to filter any five to ten point noise spike (irrespective of the magnitude) effects, interference from other devices etc. before the start combustion that might appear in the cylinder pressure trace on account of the background noise. Fig 5.6 shows that the filtered output is able to reconstruct the pressure trace in the part obscured by abrupt background noise.

The five-point moving average filtering algorithm identifies the start and end of the abrupt noise spike and replaces the spike in between those sample points with the average of the noise start and end point. This was feasible because of negligible difference between the noise

spike start and end point for cylinder pressure acquisition at 0.1 degree CA resolution. Fig 5.6 shows that the random noise spike in the cylinder pressure trace was attenuated completely.

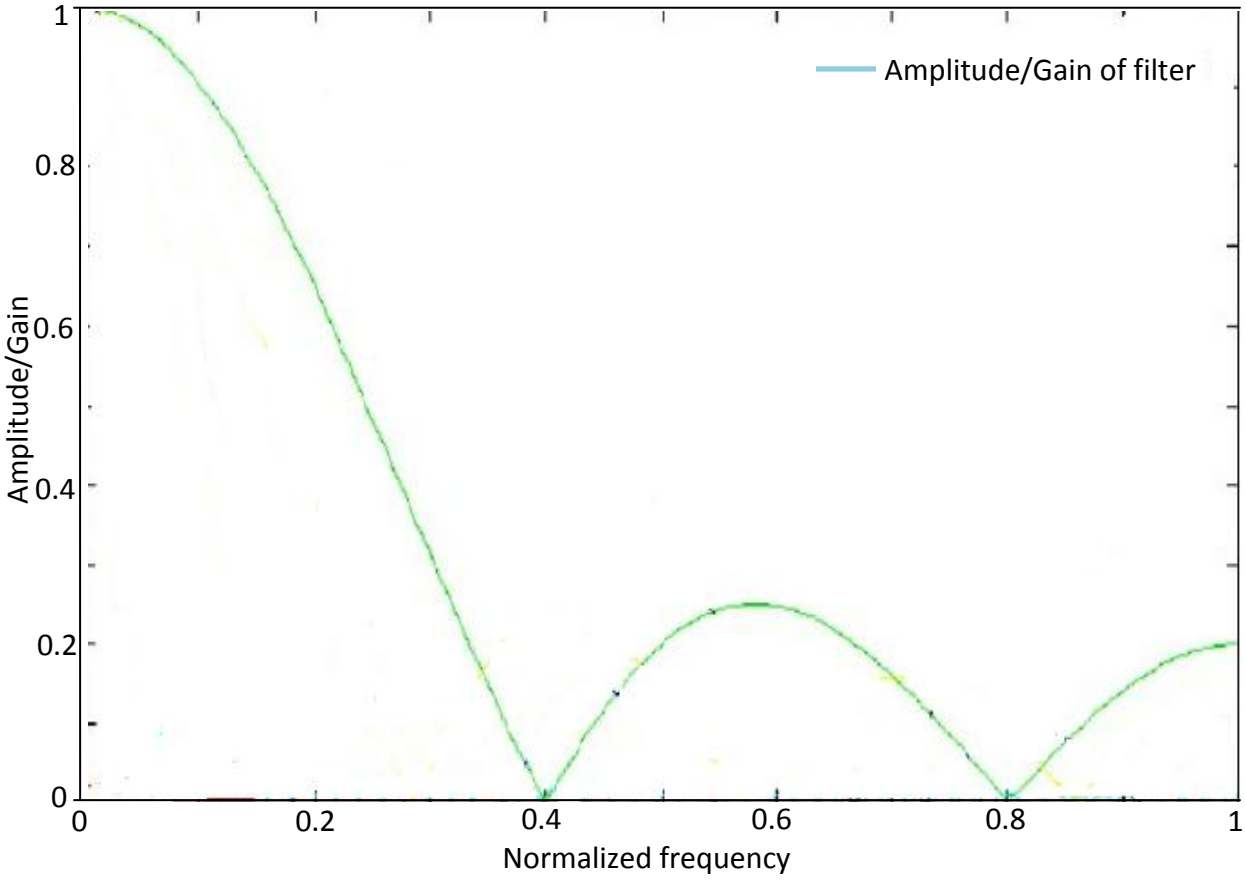

Fig 5.5: Frequency response of 5-point moving average filter

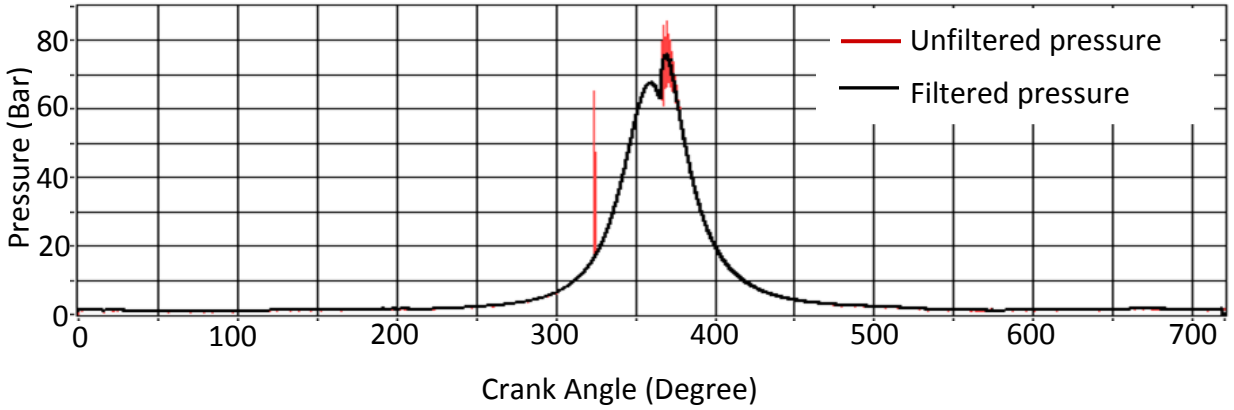

Fig 5.6: Filtering of random noise spike in the cylinder pressure before start of combustion

5.3.3. Proposed filter

The proposed filter employs an algorithm to identify the start of combustion and switches between the two aforesaid filters. The five-point moving average filter starts operating from the beginning of the cylinder pressure cycle and shifts to the forward and reverse order five Butterworth filter once the start of combustion occurs in the cylinder pressure trace. The switch from the five point moving average filter to the forward and reverse filter allows the filtered output to track the abrupt jump in cylinder pressure that is caused by start of combustion.

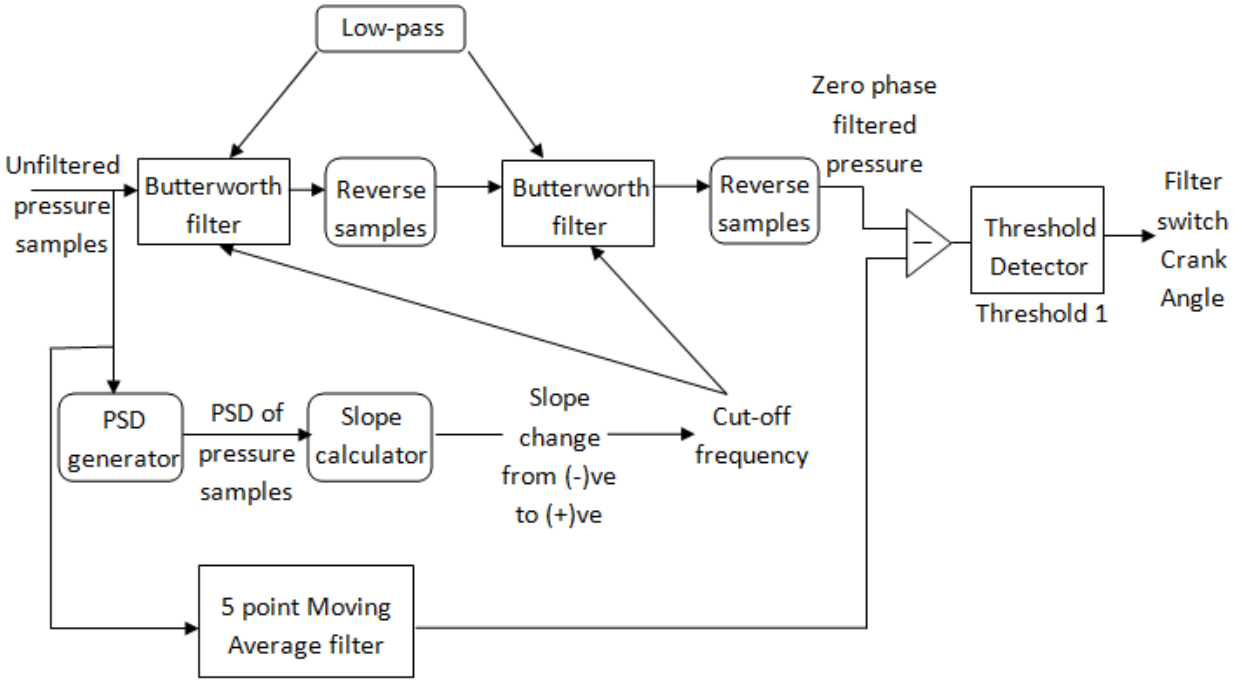

Fig 5.7: Block diagram of the proposed filter

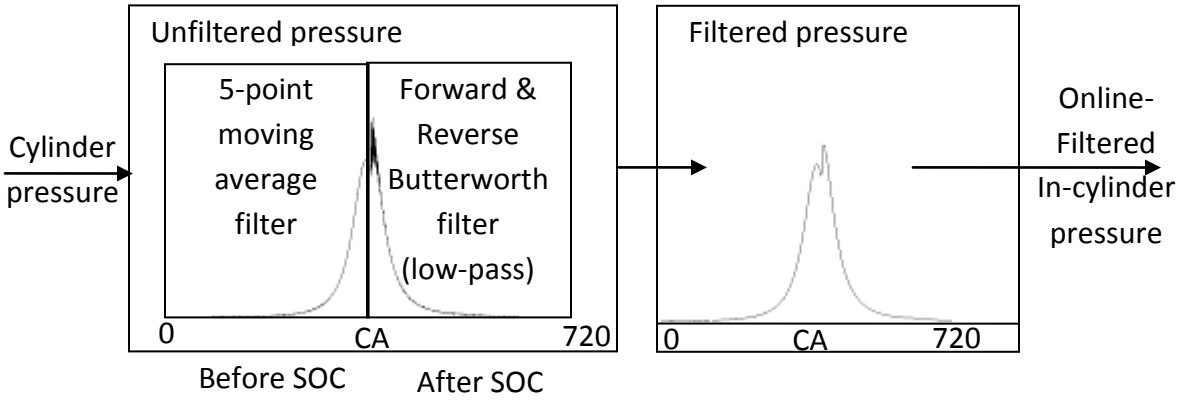

Fig 5.8: Block Diagram of the operating principle of the proposed filter

As shown in Fig 5.7, the start of combustion is identified by calculating the difference between the moving-average filtered and zero-phase filtered outputs. Once the difference crosses a certain threshold, (1 bar since the filter does not operate until this difference for the motoring curve exceeds 1 bar) the filter switches. Due to an intelligent switching between the filters just after the start of combustion, it is possible to avoid the shift in the filtered pressure trace.

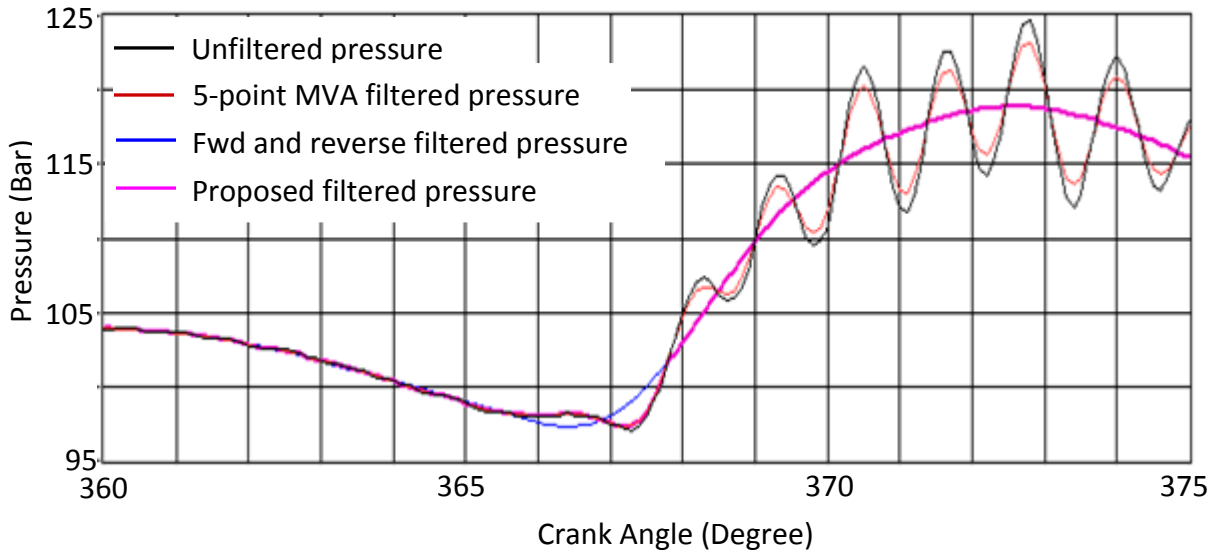

Fig 5.9: Comparison of different filters in tracking the start of combustion

5.4. Decomposition of in-cylinder pressure

First, an attempt was made to characterize the in-cylinder pressure based on the occurrences during an engine run. As part of analysis of the in-cylinder pressure data on a cycle-by-cycle basis, a technique of in-cylinder pressure decomposition [11] is used. Similar analysis is done for both the engine pressure data. The cylinder pressure curve was decomposed into three principal components namely motoring curve (pressure rise caused by the piston movement), combustion curve (caused by the combustion) and the high frequency noise (consisting of access passage resonance, chamber resonance and piston slap etc.). The combustion plus noise trace can be obtained by subtracting the motoring curve from the unfiltered pressure trace. The combustion-only pressure trace is obtained by subtracting the motoring curve from the filtered pressure trace. The noise curve is therefore obtained by subtracting the combustion-only curve from the combustion-plus-noise curve. The cylinder pressure curve is thus decomposed into the motoring, combustion-only and the unaccounted noise curves.

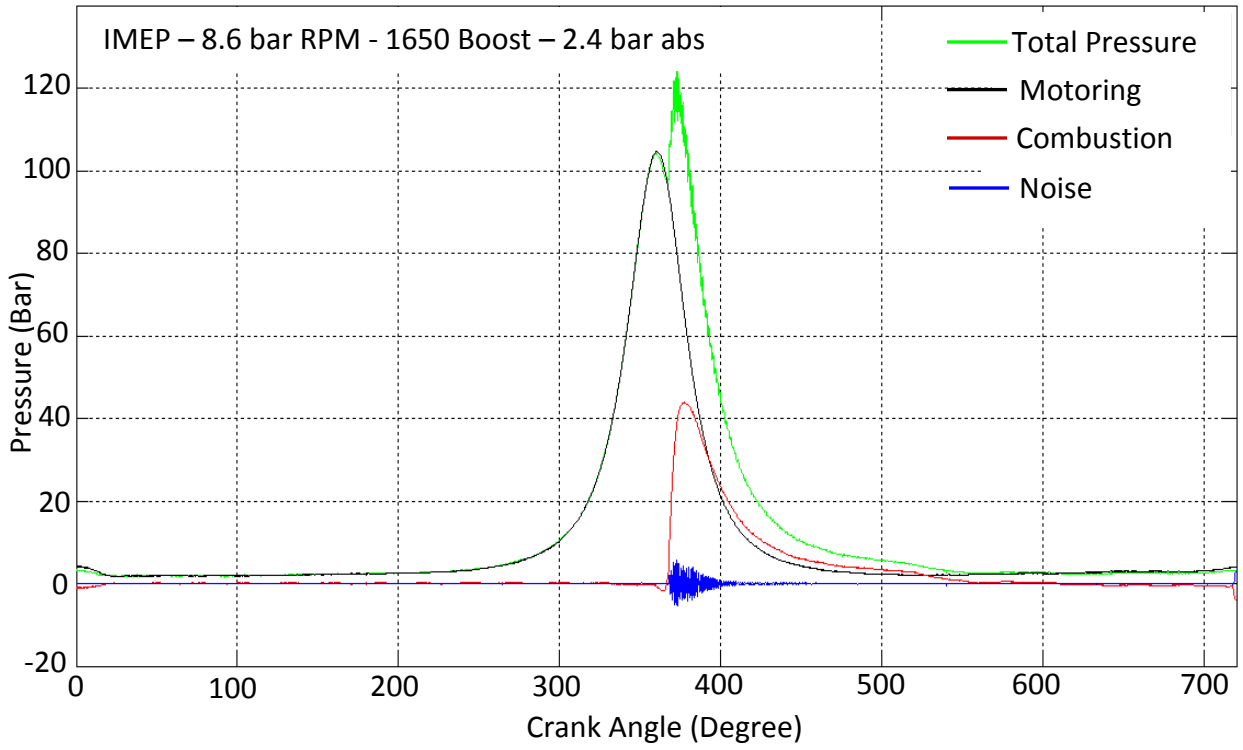

Fig 5.10: Decomposition of the unfiltered pressure trace (Single cylinder engine)

Let P, M, C and N represent the unfiltered pressure, motoring, combustion-only and the noise signal respectively as functions of crank angle (θ). Using the pressure decomposition principle, the unfiltered pressure P can be expressed as

$$P(\theta) = M(\theta) + C(\theta) + N(\theta) \tag{5.3}$$

Fig 5.10 shows the different segregated pressure signal components. However, a better way of analysis of the different components is to obtain the spectral components for each of the segregated parts. This gives an idea about the distribution of signal and noise power over the entire frequency range and the effect of engine load, speed and boost on each of the components esp. noise. Similar analysis is done on both the engines in the laboratory to obtain the PSD of the cylinder pressure under different engine run conditions. However, results obtained from one particular test run condition corresponding to both the engines are included here. An important point to note here is that the peak noise frequency component remains unchanged irrespective of the engine run conditions for each of the engines.

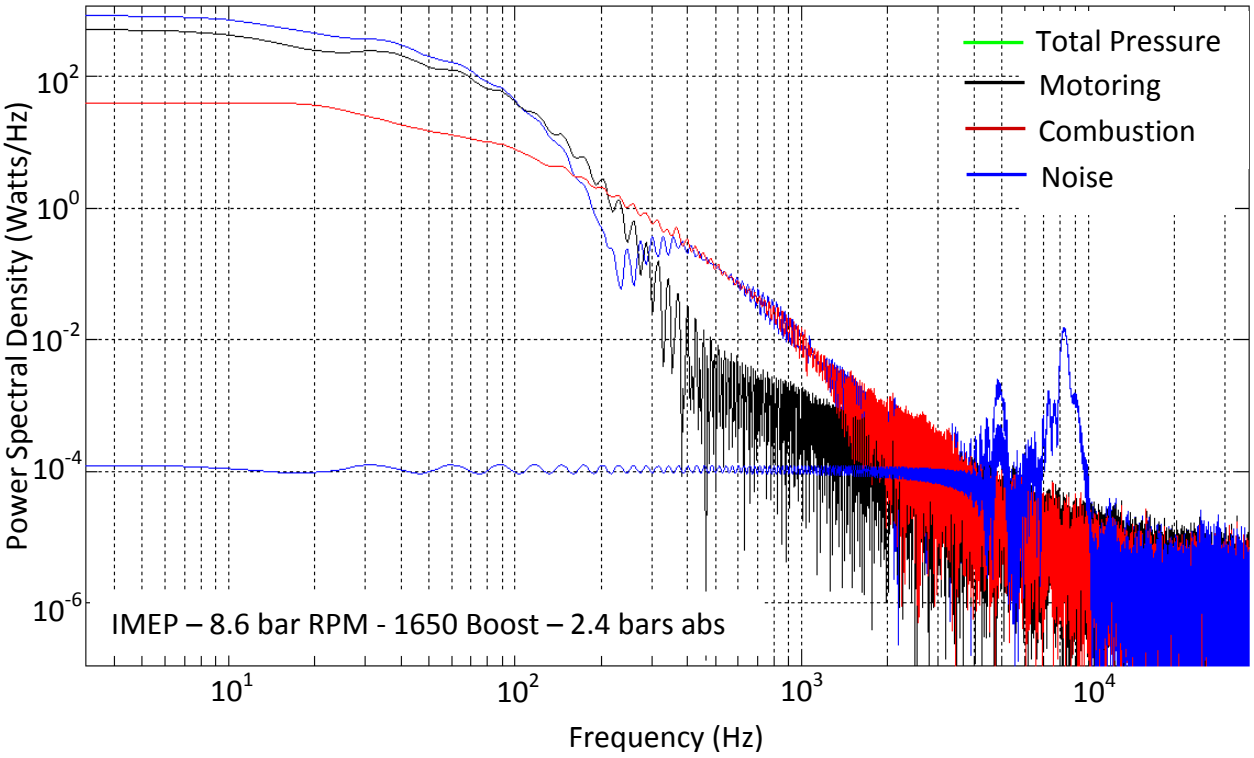

Fig 5.11: Decomposition of the unfiltered pressure PSD (Single cylinder engine)

From Fig 5.11, it is evident that the low-frequency spectral components up to around 180 Hz are dominated by the motoring curve (pressure change effected by piston movement). The mid-frequency components from 180 Hz to 3.1 kHz are dominated by the combustion-only signal spectrum. The spectral components higher than 3.1 kHz are dominated by the unaccounted noise. As the noise components dominate from 3.1 kHz, choice of the cut-off frequency for this particular test run is validated. For the single cylinder engine, it was observed that the peak noise frequency is around 8.5 kHz. This peak in the noise spectrum of the single cylinder engine remains same for all the analysis results irrespective of the engine run conditions such as engine speed, load and boost. However, this particular spectral distribution depends on the engine mount which is hereby assumed to be constant. Similar analysis is done for the Ford Puma engine to find the robustness of this methodology.

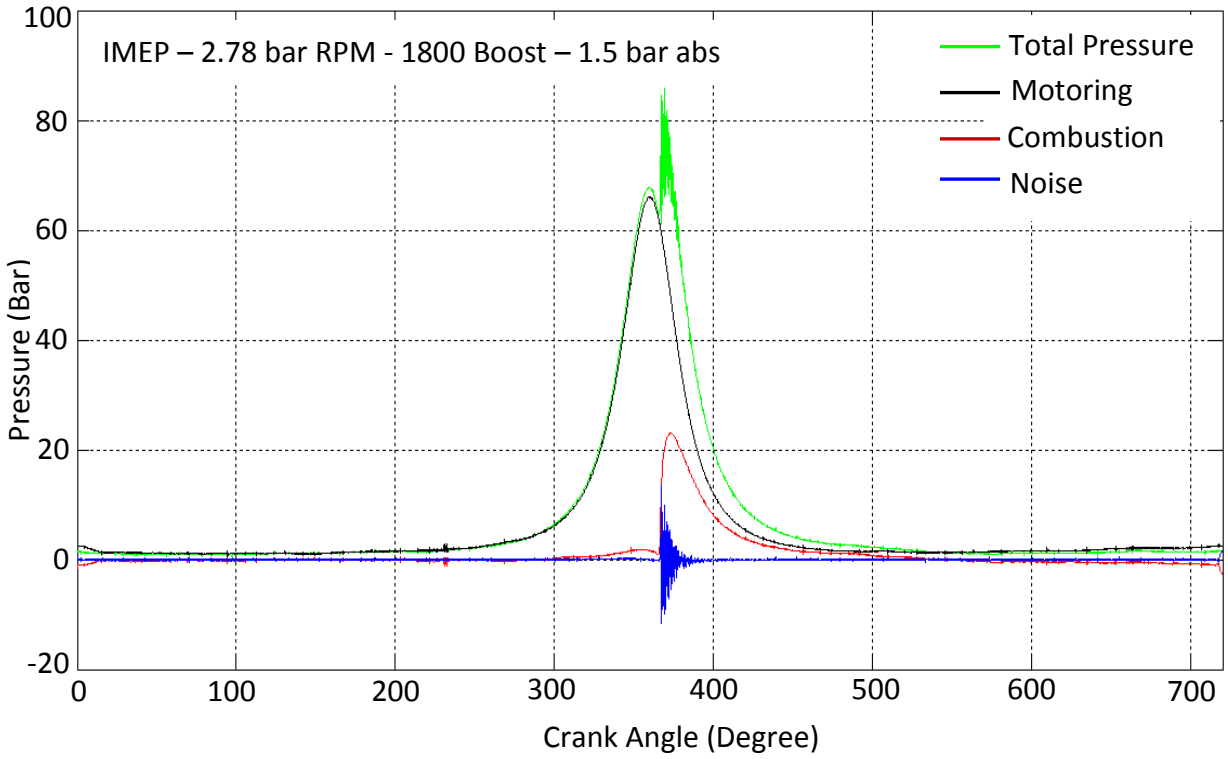

Fig 5.12: Decomposition of the unfiltered pressure trace (Ford engine)

Spectral analysis (along with segregation) of the Ford engine cylinder pressure trace in Fig 5.13 shows results in accordance of the results obtained by analyzing the single cylinder engine. However, the numerical values vary on account of the difference of the engine specifications. The motoring curve components dominate up to a frequency of exactly 200 Hz (which was 180 Hz for the single cylinder engine). The combustion-only signal components have the maximum power from 200 Hz till 3.42 kHz. The unaccounted noise dominates from the frequencies above 3.42 kHz. This spectral analysis in turn validates the choice of cut-off frequency for the filter. From the above figure the peak noise frequency was around 14.5 kHz.

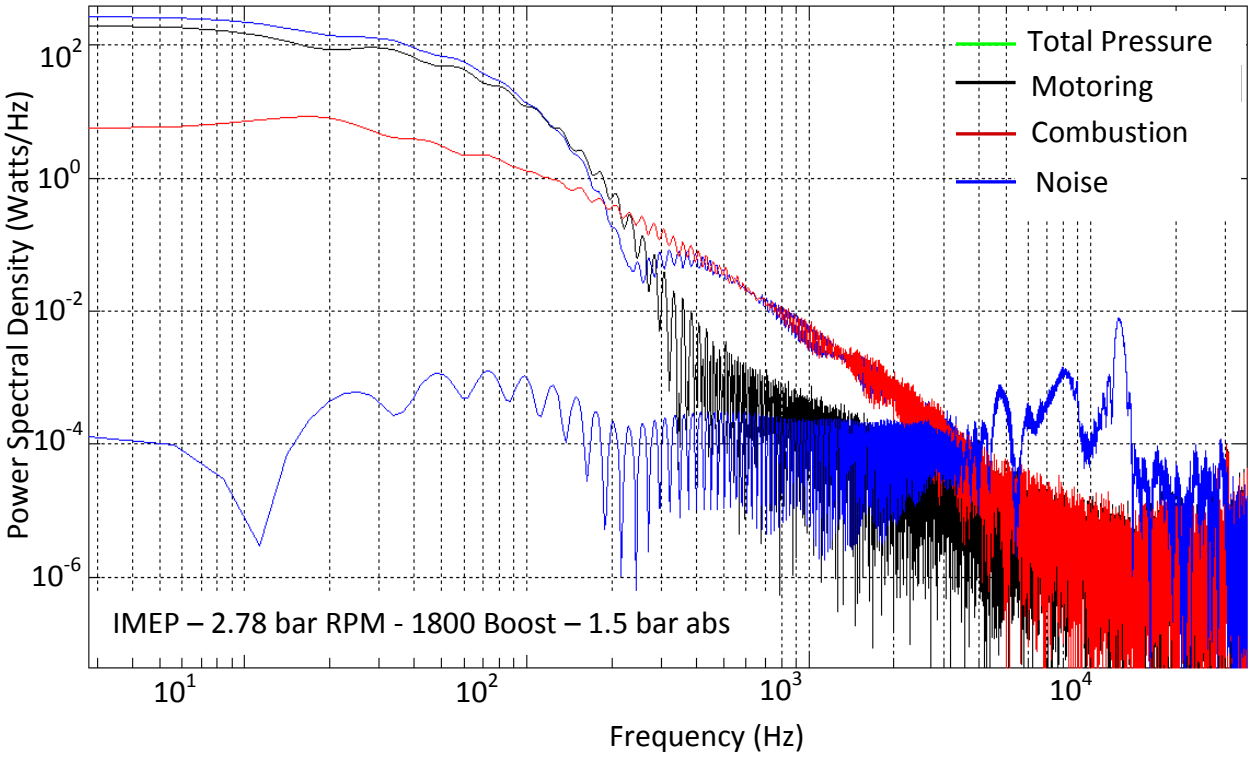

Fig 5.13: Decomposition of the unfiltered pressure PSD (Ford engine)

5.5. Application of the filter on cylinder pressure and heat release rate (HRR) curve

The proposed filter is tested on multiple engine run conditions e.g. speed (1200-3000 rpm), load (3-10 bar) and different combustion modes e.g. HCCI, LTC for both the engines. The filtered heat release rate curve for both the engines is also shown in the subsequent plots.

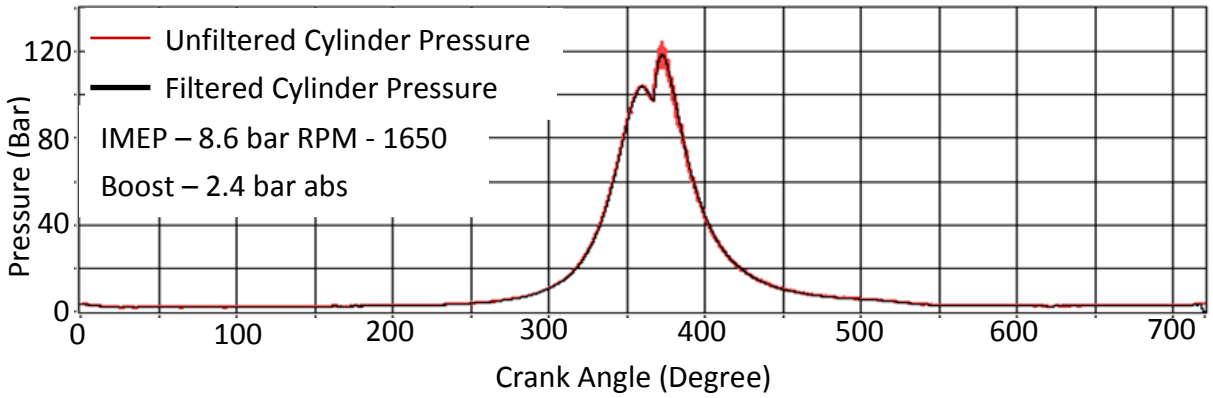

Fig 5.14: Filtered and the unfiltered cylinder pressure trace (Single cylinder engine)

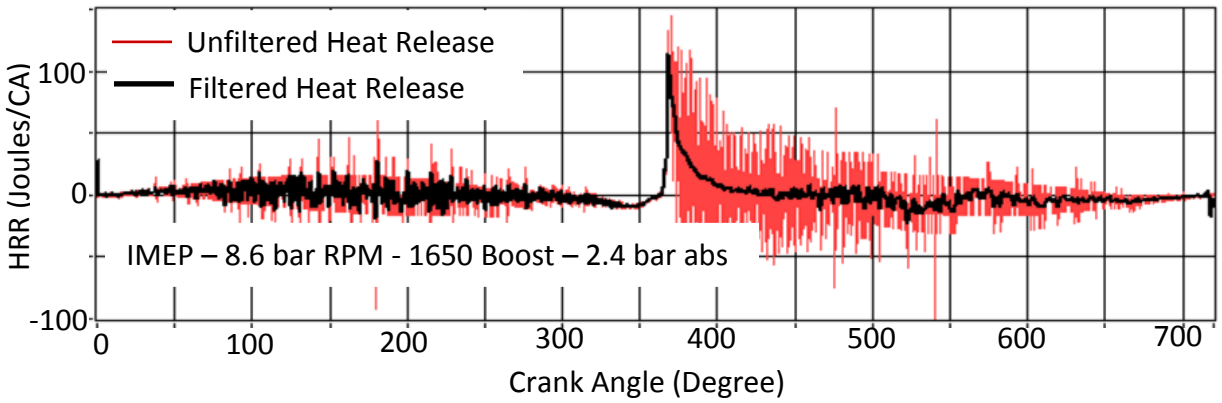

Fig 5.15: Filtered and the unfiltered heat release rate (Single cylinder engine)

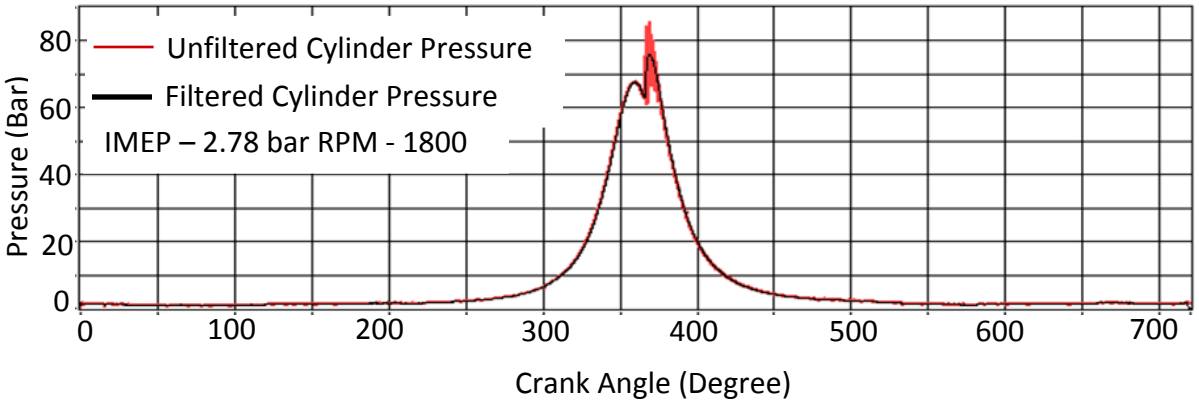

Fig 5.16: Filtered and the unfiltered cylinder pressure trace (Ford engine)

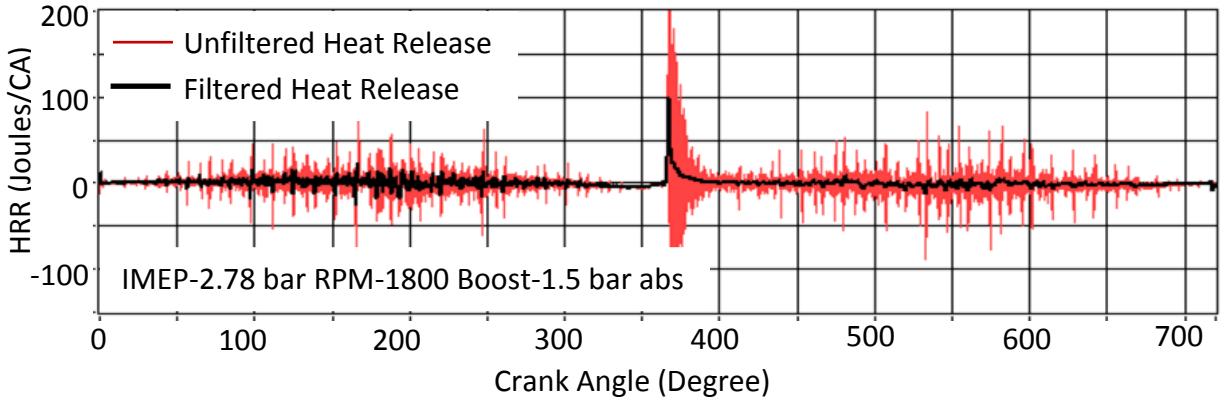

Fig 5.17: Filtered and the unfiltered heat release rate (Ford engine)

The filtering is done based on the 7200 sample points obtained per cycle which gives better leverage in terms of filtering. However, the filtered output is represented with respect to the

crank angle i.e. 720 points. Filtering at 0.1 degree CA resolution leads to an improved filtered output. At present, an online down-sampled heat release curve is displayed while running the engine. Fig 5.17 and Fig 5.18 show that filtering in the 7200 point domain helps to eliminate noise and retain the information content of the signal some of which might be lost while down-sampling the signal.

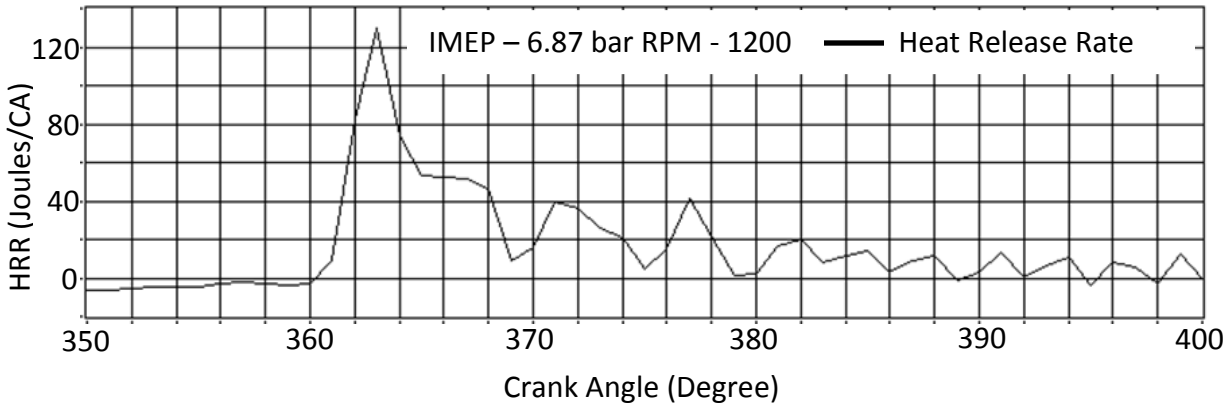

Fig 5.18: Down-sampled heat release rate (Single cylinder engine)

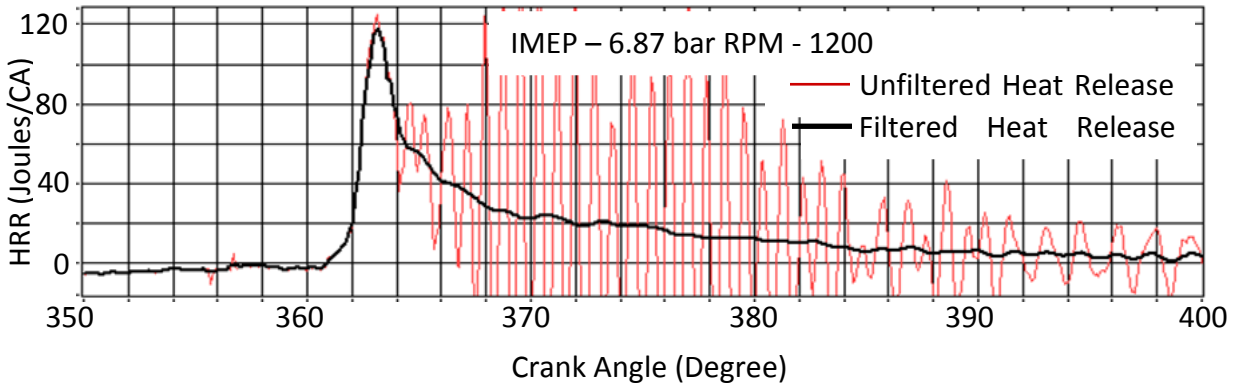

Fig 5.19: 7200 point filtered heat release rate (Single cylinder engine)

5.6. Transient speed analysis and cylinder pressure analysis post interpolation

The engine speed does not remain constant over one cylinder pressure cycle. If engine runs at 1500 rpm, the engine does not maintain this particular speed during the entire period of engine run. Consequently, the acquired cylinder pressure samples are not equispaced i.e. the sample intervals vary from one sample to the other. Therefore, the analysis done based on this kind of

recording can give erroneous results as all calculations are based on the assumption that the sample points are equispaced. A Labview code is used to record the transient engine speed and the sample interval for all the 7200 points on an online (cycle-by-cycle) basis. Fig 5.20 shows the engine speed fluctuation over one pressure cycle of Ford Puma engine.

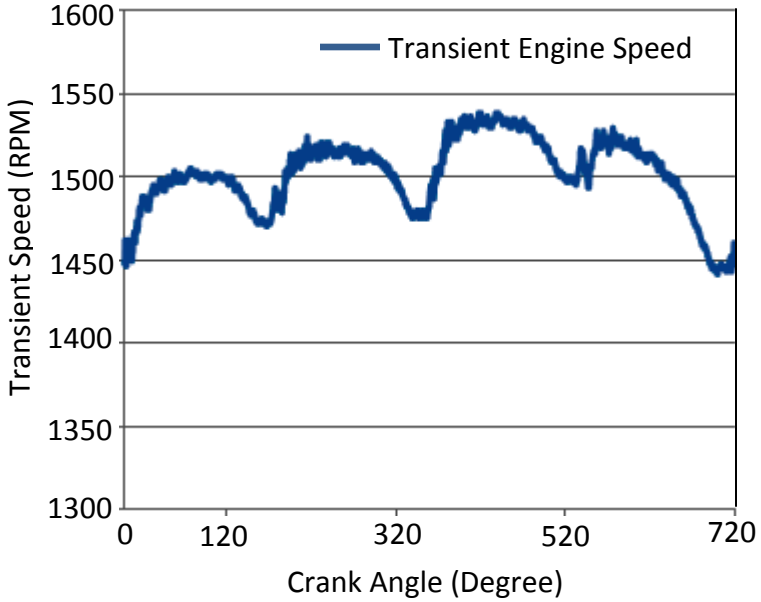

Fig 5.20: Transient engine speed in a cylinder pressure cycle (Ford Engine)

Although the engine is running at 1500 rpm, it can be clearly seen the engine speed ranges from a peak of 1540 to a low of 1450 within a single cylinder pressure cycle. A possible solution to this is to interpolate the pressure signal using Matlab so as to generate equispaced sample points in the time domain. For the Ford engine, one single cycle takes a total of 79945 microseconds (approx.) while running at 1500 rpm. A sampling frequency of 125 kHz which is higher than the normal sampling frequency (obtained by assuming fixed engine speed which is 90 kHz) is used to interpolate the pressure trace in the time domain. Apart from obtaining equispaced samples in the time domain, interpolated pressure curve also provides some additional information because of its higher sample resolution (10,000 samples) compared to 7200 samples in the geometric domain.

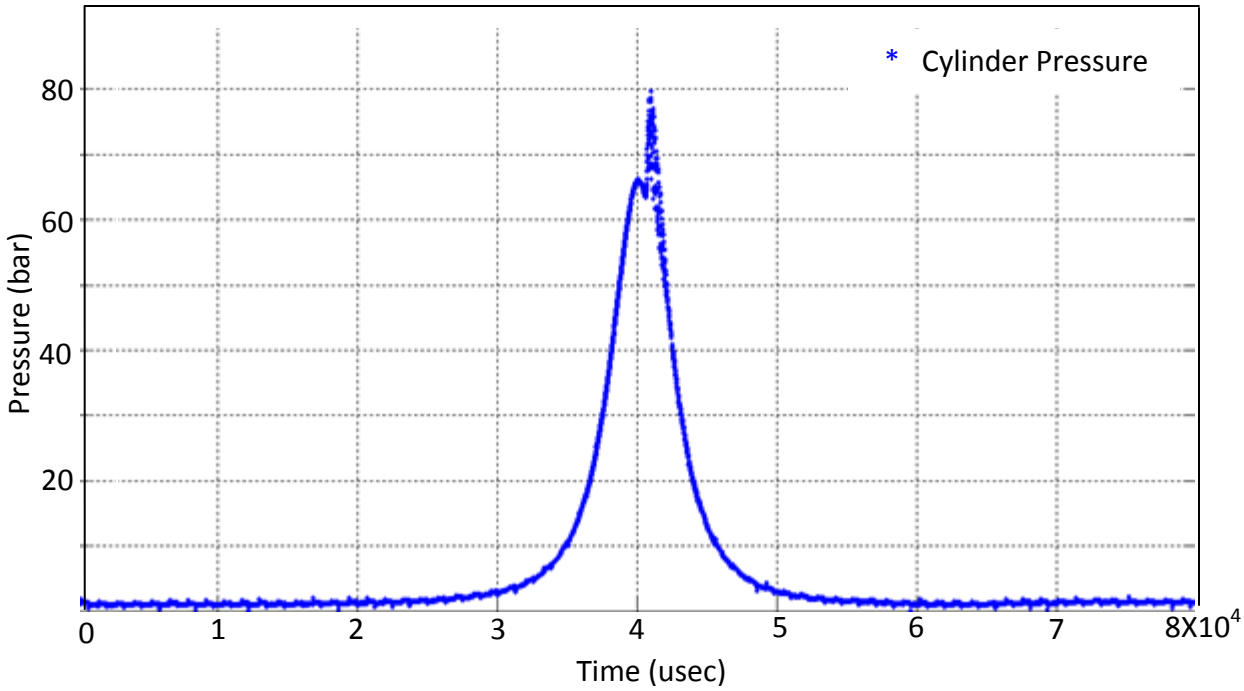

Fig 5.21: Cylinder pressure cycle post interpolation (Ford Puma engine)

5.7. Cylinder pressure noise spectral analysis and characterization

The cylinder pressure trace obtained in the time domain is analyzed by using Fast Fourier Transform (FFT). Noise cancellation of the cylinder pressure trace is done by using the proposed filter. After segregation of the noise components, noise analysis reveals close correlation between the peak noise frequency and the access passage frequency calculated for the single cylinder engine using SAES [20]. From Fig 5.11, it was observed that peak noise frequency exists around 8.5 kHz. The pressure trace for the single cylinder engine is simulated using SAES [20] by providing all the necessary engine run conditions. An attempt was made to correlate the peak noise frequency with the frequency of the sound waves generated due to access passage resonance. In order to measure the speed of sound within the combustion chamber, the gaseous composition of the cylinder chamber has to be known which is determined iteratively by using SAES [20]. By specifying the engine operating conditions, cylinder pressure, in-cylinder temperature, adiabatic coefficient γ, concentration of carbon dioxide (CO_2), oxygen (O_2), nitrogen (N_2) and water vapor (H_2O) simulations can be obtained from SAES [20].

The speed of sound was calculated by using the formula for the speed of sound in gases [24] i.e.

$$c = \sqrt{\gamma R_m T} \tag{5.4}$$

where c is the speed of sound in gases, γ is the adiabatic coefficient i.e. the ratio of specific heat at constant pressure to constant volume, R_m is the universal molar gas constant and T is the mean cylinder temperature. It is assumed that the temperature remains constant, ideal gas law and adiabatic condition holds. For the sake of simplicity, it is assumed that these conditions hold inside the combustion chamber.

The first harmonic of the standing wave in the access passage [12] is obtained from the formula

$$f = \frac{c}{4l} \tag{5.5}$$

where *f* is the access passage frequency, c is the speed of sound and *l* is the length of the duct or access passage. Based on the engine specifications provided in Table 4.1, the duct length (*l*) for the single cylinder engine is 23 mm. First, an entire single cylinder engine pressure cycle is simulated using SAES [20] and the concentration of each of the gases is used to determine the value of the universal molar gas constant for the gaseous mixture. The peak temperature point within the cycle is chosen as the sample point of interest. All measurements are done for this particular sample point. The speed of sound for this point is found to be 790 m/sec (approx). Therefore, using the formula mentioned above, the resonant frequency comes out to be 8.57 kHz. This is very close to the peak noise frequency in the spectral analysis of the cylinder pressure trace as shown in figure 5.11. Therefore, it can be concluded that the peak noise frequency can be attributed to the access passage resonant frequency caused by acoustic resonance.

However, a similar assessment is not possible for the Ford Puma engine since no information is available regarding the access passage length (for transducer mounting). But it is possible to estimate the approximate length of the duct in the Ford engine. Figure 5.13 shows that the peak noise frequency exists at around 14.5 kHz. SAES [20] is used to simulate the engine

gaseous concentration for the entire pressure cycle. Using the same method as used for the single cylinder engine, value of the universal molar gas constant is derived and the speed of sound is calculated for all the sample points. The speed of sound is averaged over all the sample points in the entire cycle (586 m/sec approx). Using Equation 5.5, the value of the duct length is obtained by averaging over all the sample points in the entire cycle is 7 mm (approx).

Therefore, it can be concluded that the unaccounted noise can be primarily attributed to the access passage frequency with the peak noise power showing high correlation with the duct resonant frequency. However, smaller noise peaks surrounding the big one can be attributed to background noise such as EMI, electrical connections and wiring, combustion noise, chamber resonance etc. An increase in the engine load caused a shift in the noise frequency components. This is mostly because of the effect of combustion noise in the high frequency zone of the spectral components of the cylinder pressure signal.

6. CONCLUSION AND FUTURE WORK

The effect of non-flush mounted pressure transducer on cylinder pressure was studied in detail in this work. Apart from non-flush mounting of the transducer, the cylinder pressure is obscured by pulsations caused by electro-magnetic interference, electrical connections and wiring and combustion noise among other factors. Vibration of the gases inside the cylinder chamber tend to induct errors in the cylinder pressure curve and consequently in the heat release curve. Important parameters related to combustion such as SOC, EOC, maximum rate of pressure rise, IMEP etc. that are calculated from the heat release curve derived from noisy cylinder pressure curve also become erroneous which is highly undesirable for combustion analysis. This work includes the design of an online filter in order to nullify the effect of unaccounted noise in the cylinder pressure trace. A concurrent display of filtered cylinder pressure and heat release provides leverage for an improved control over the test conditions with considerably less computational overhead as compared to post-processing of the data. A brief summary of the work done is given below.

1. Segregation of the different signal components of the cylinder pressure trace was done so as to obtain the power spectral density curves for the motoring-only, combustion-only and the unaccounted noise. It was observed that the high frequency components are dominated by the unaccounted noise whereas the mid-frequency components are dominated by the combustion-only curve and the motoring signal spectrum dominates the low frequency zone.

2. A low-pass forward and reverse order five Butterworth filter is used in conjunction with a five point moving average filter to attenuate the high frequency noise from the cylinder pressure trace. The filter identifies the start of combustion and switches from the five-point moving average filter to the forward and reverse Butterworth filter just after the start of combustion. Therefore, the filter is able to track the abrupt increase in the cylinder pressure trace. The moving average filter is also capable of nullifying the

effect of any random noise in the cylinder pressure trace before the start of combustion. The cut-off frequency of the filter is determined on an online basis (cycle by cycle) and therefore no preset cut-off frequency for the filter is necessary. The cut-off frequency for the filter changes with change in the engine operating conditions and eventually it might vary from cycle to cycle. Most of the filters designed so far in the literature has either not been tested on all engine operating conditions (speed and load) or are only an extension of the offline filters where filter parameters were mostly preset. This filter was tested on the cylinder pressure trace over different engine speeds in the range of 1000-3000 rpm and engine loads of 3-10 bar.

3. Interpolation of the cylinder pressure was done in order to account for the variations of engine speed within a single cycle of the cylinder pressure. Since the engine speed varies within a single cycle, the sample points for a fixed sampling frequency are not equally spaced over time i.e. the sampling interval varies from one sample to the other. So, the analyses made based on these samples could be erroneous. The sample intervals were recorded as part of the transient engine speed analysis. The cylinder pressure trace was interpolated so as to obtain higher number of equally spaced points in a single cycle of the time domain. An increased number of sample points gives a better frequency resolution in FFT analysis and an equal sampling interval ensures the quality of the subsequent analyses.

4. The noise in the cylinder pressure trace was characterized and the principal source was identified as the pulsations caused by the standing waves in the access passage connecting the pressure transducer. It was shown for the single cylinder engine that the peak noise frequency component in the PSD diagram of the cylinder pressure is highly correlated with the duct resonant frequency. However, calculations were done based on the duct length for the single cylinder engine. But, no information is available regarding the mounting scheme of the pressure transducer in the Ford Puma engine. Therefore, similar calculation as mentioned above was not possible in this work. However,

assuming that the correlation that was established for the single cylinder engine holds for the Ford engine, backtracking was done to find a possible length of the duct or the access passage in the Ford engine.

The pressure decomposition technique helped in segregating noise components from the in-cylinder pressure trace. It was observed that the energy content in the noise signal relative to that in the motoring signal governs the sound quality of combustion noise. Further studies might make it possible to achieve optimal combustion control by means of the development of optimal injection strategies fulfilling emission reduction and performance requirements in Diesel engines. Pollutant emission reduction can be achieved by activating or deactivating pilot injection keeping the combustion noise under a certain threshold.

This work can be further extended to analyze the sensitivity of combustion noise or resonance to changes in engine parameters such as injection strategy, bowl geometry, EGR, coolant temperature, etc. [11]. The filtered cylinder pressure output can be used to validate different mathematical simulation models. Characterization of noise into various components might lead to the design of new combustion strategies so as to keep the noise level within a preset limit.

REFERENCES

1. W.T.Lyn, A.J.Stockwell, C.H.T.Wang, "Accuracy in Cylinder Pressure Measurement" Proceedings of the Institution of Mechanical Engineers, Conference Proceedings 1965 180:8.
2. D.T.Hountalas, A.Anestis, "Effect of Pressure Transducer Position on Measured Cylinder Pressure Diagram of High Speed Diesel Engines" Energy Convers. Mgmt Vol. 39, No. 7, pp 589-607,1998
3. Nagao Fujio, Ikegami Makato, "Errors of an Indicator due to a Connecting Passage", JSME 621.43.018.86
4. J.P. Elson, W. Soedel, "Criteria for the Design of Pressure Transducer Adapter Systems", International Compressor Engineering Conference, 1972.
5. F. Payri, J.M. Lujan, J. Martin, A. Abbad, "Digital Signal Processing of In-cylinder Pressure for Combustion Diagnosis of Internal Combustion Engines", Mech. Syst. Signal Pr. 24 (2010) 1767-1784.
6. R.Douglas, R.J.Kee, B.P.Carberry, "Analysis of Chamber Pressure Data in Two-stroke Engines", SAE Paper 972972, 1997.
7. S.X.Shi, H.Z.Sheng, "Numerical Simulation and Digital Signal Processing in measurements of Cylinder Pressure of Internal Combustion Engines", IMechE C20/87 (1987) 211-218.
8. A.Savitzky, M.J.E.Golay, "Smoothing and Differentiation of Data by Simplified Least Squares Procedures", Anal. Chem. 36 (1964) 1627-1639.
9. F.Payri, P.Olmeda, C.Guardiola, J.Martin, "Adaptive Determination of Cut-off frequencies for filtering the In-cylinder Pressure in Diesel Engines Combustion Analysis", Mech. Syst. Signal Pr. 31 (2011) 2869-2876.
10. E.L.Kosarev, E.Pantos, "Optimal smoothing of 'noisy' data by Fast Fourier Transform", J.Phys. E: Sci. Instrum. 16 (1983) 537-543.
11. F.Payri, A.Broatch, B.Tormos, V.Marant, "New Methodology for In-cylinder Pressure Analysis in Direct Injection Diesel Engines - application to combustion noise", Meas. Sci. Technol.16 (2005) 540-547.
12. U.Asad, Raj Kumar, Xiaoye Han, Ming Zheng, "Precise Instrumentation of a Diesel Single-cylinder Research Engine ", Measurement 44 (2011) 1261-1278.

13. A.Hirose, K.E.Lonngren, “Introduction to Wave Phenomena”, John Wiley and Sons, 1985.
14. J.A.Eng, “Characterization of Pressure Waves in HCCI Combustion”, SAE Technical Paper Series 2002-01-2859.
15. M.F.J.Brunt, C.R.Pond, “Evaluation of techniques for absolute cylinder pressure correction”, SAE Paper 9700369, 1997.
16. M.T.Wlocardyk, “High accuracy glow-plug integrated cylinder pressure sensor for closed loop engine control”, SAE Paper 2006-01-0184, 2006.
17. G.Phillips, P.Taylor, “Theory and applications of Numerical Analysis”, second ed., Elsevier Academic Press, London, 1996.
18. M.F.J.Brunt, G.Gordon.Lucas, “The effect of Crank Angle resolution on cylinder pressure analysis”, SAE Paper 910041 1991.
19. J.B.Heywood, ”Internal Combustion Engine Fundamentals”, Mc-Graw-Hill, USA, 1988.
20. M.Zheng, G.T.Reader, “ Synthetic Atmospheric Engine Simulations (SAES)”, 1994.
21. http://fusionone.ca/wp-content/uploads/2011/09 , Accessed on May 24, 2012.
22. Intertechnology Inc. http://www.intertechnology.com/Kistler/Pressure_Model_6052B1.htm , Accessed on May 10, 2012.
23. Piezocryst Product Portfolio, Combustion Analysis Sensors, Graz, 2007, http://www.piezocryst.com/downloads/Product_Overview_Automotive_Sensors.pdf, Accessed on May 15, 2012.
24. M.Luperta, O. Armas, J.J.Hernandez, “ Diagnosis of Diesel combustion from in-cylinder pressure signal by estimation of mean thermodynamic properties of the gas”, Applied Thermal Engineering 19 (1999) 513-529.

VITA AUCTORIS

NAME:	Koustav Dey
PLACE OF BIRTH:	Kolkata, India
YEAR OF BIRTH:	1988
EDUCATION:	Kalyani Government Engineering College, W.B., India B.Tech Electronics and Communication Engineering 2010
	R.K.Mission Vidyalaya, Narendrapur, W.B., India 2006